

Reactions of the Phosphinidene-Bridged Complexes [Fe₂(η⁵-C₅H₅)₂(μ-PR)(μ-CO)(CO)₂] (R = Cy, Ph, 2,4,6-C₆H₂^tBu₃) with Diazoalkanes. Formation and Rearrangements of Phosphadiazadiene-Bridged Derivatives[†]

M. Angeles Alvarez, M. Esther García, Rocío González, and Miguel A. Ruiz*

Departamento de Química Orgánica e Inorgánica/IUQOEM, Universidad de Oviedo, E-33071 Oviedo, Spain

Received April 26, 2010

The phosphinidene complexes [Fe₂Cp₂(μ-PR)(μ-CO)(CO)₂] (Cp = η⁵-C₅H₅; R = Cy, Ph, Mes*; Mes* = 2,4,6-C₆H₂^tBu₃) react readily with diazoalkanes N₂CR'R'' (R' = H, R'' = H, CO₂Et, SiMe₃; R' = R'' = Ph) in dichloromethane solution at room temperature or below to give the corresponding *P:P*-bridged phosphadiazadiene derivatives [Fe₂Cp₂(μ-RPN₂CR'R'')(μ-CO)(CO)₂] (**2**) with high yield. The diazomethane derivative (Fe–Fe = 2.6198(6) Å) is protonated selectively with HBF₄·OEt₂ at the P-bound nitrogen atom to yield the aminophosphide derivative [Fe₂Cp₂(μ-CyPNHNCH₂)(μ-CO)(CO)₂](BF₄) (Fe–Fe = 2.6126(5) Å). Compounds **2** decompose upon heating in toluene solution at 363 K to give the dimer [Fe₂Cp₂(CO)₄] as the only organometallic product. The same result was obtained when irradiating with visible–UV light toluene solutions of the phenylphosphinidene-derived compounds. In contrast, relatively selective decarbonylations could be induced photochemically when R = Cy, Mes*. The reaction products, however, were strongly dependent on the nature of all substituents present in compounds **2**. The diazomethane derivative yielded a mixture of the *P:N*-bound phosphadiazadiene complex [Fe₂Cp₂(μ-CyPN₂CH₂)(μ-CO)₂] (major) and the phosphalkene derivative [Fe₂Cp₂(μ-CyPCH₂)(μ-CO)(CO)] (minor). In contrast, the ethyldiazoacetate derivative gave the paramagnetic complex [Fe₂Cp₂{μ-CyPN₂CH(CO₂Et)}(μ-CO)(CO)], possibly containing a *μ-P:P,C*-phosphadiazadiene ligand, which upon chromatography fully rearranges into the aminophosphide-iminoacyl complex [Fe₂Cp₂{μ-CyPNHNC(CO₂Et)}(μ-CO)(CO)] (Fe–Fe = 2.6261(8) Å), possibly through a protonation/deprotonation sequence on the alumina surface. The trimethylsilyldiazomethane derivative instead gave directly the analogous aminophosphide-iminoacyl complex [Fe₂Cp₂{μ-CyPN(SiMe₃)NCH}(μ-CO)(CO)], now resulting from an unusual 1,3-shift of the SiMe₃ group along the ligand backbone. Finally the photochemical treatment of the ethyldiazoacetate derivative of the supermesitylphosphinidene substrate gave the complex [Fe₂Cp₂{μ-Mes*PN₂CH(CO₂Et)}(μ-CO)₂] (Fe–Fe = 2.514(1) Å), containing a *P:N*-bridged phosphadiazadiene ligand bound to the dimetal center in a novel coordination mode, this involving the P-bound nitrogen atom, instead of the C-bound nitrogen.

Introduction

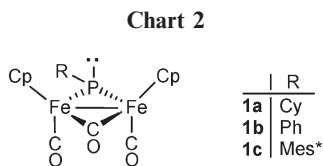
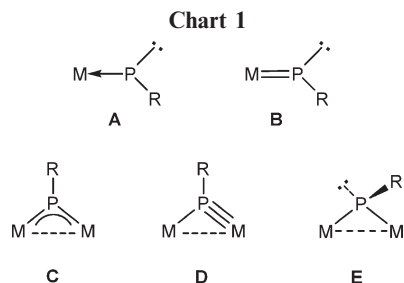
The study of phosphinidene complexes is a fruitful area of research within the current organometallic chemistry.¹ Most of the work in this active area has been carried out so far on the bent-terminal complexes, these having a nonbonding electron pair at a low-coordination phosphorus atom and a metal–phosphorus bond that can be described as essentially single or double, depending on the metal environment (**A** and **B** in Chart 1), all of which makes these complexes highly reactive toward a great variety of unsaturated organic molecules, then

making them useful in the synthesis of numerous organophosphorus compounds.¹ In contrast, the chemistry of binuclear complexes having phosphinidene bridges has remained comparatively little explored until recently, even though the presence of multiple M–P bonds or lone pairs at phosphorus in their different coordination modes (**C** to **E** in Chart 1) should

[†] Part of the Dietmar Seyferth Festschrift. This work is dedicated to Prof. Dietmar Seyferth, in recognition for his outstanding contribution to organometallic chemistry, both as an original researcher and as an efficient and kind editor of the prime specialized journal in the field.

*To whom correspondence should be addressed. E-mail: mara@uniovi.es.

(1) Reviews: (a) Aktas, H.; Slootweg, J. C.; Lammerstma, K. *Angew. Chem., Int. Ed.* **2010**, *49*, 2. (b) Waterman, R. *Dalton Trans.* **2009**, 18. (c) Mathey, F. *Dalton Trans.* **2007**, 1861. (d) Lammertsma, K. *Top. Curr. Chem.* **2003**, *229*, 95. (e) Streubel, R. *Top. Curr. Chem.* **2003**, *223*, 91. (f) Mathey, F. *Angew. Chem., Int. Ed.* **2003**, *42*, 1578. (g) Lammertsma, K.; Vlaar, M. J. M. *Eur. J. Org. Chem.* **2002**, 1127. (h) Mathey, F.; Tran-Huy, N. H.; Marinetti, A. *Helv. Chim. Acta* **2001**, *84*, 2938. (i) Stephan, D. W. *Angew. Chem., Int. Ed.* **2000**, *39*, 314. (j) Shah, S.; Protasiewicz, J. D. *Coord. Chem. Rev.* **2000**, *210*, 181. (k) Schrock, R. R. *Acc. Chem. Res.* **1997**, *30*, 9. (l) Cowley, A. H. *Acc. Chem. Res.* **1997**, *30*, 445. (m) Cowley, A. H.; Barron, A. R. *Acc. Chem. Res.* **1988**, *21*, 81. (n) Huttner, G.; Knoll, K. *Angew. Chem., Int. Ed. Engl.* **1987**, *26*, 743. (o) Huttner, G.; Evertz, K. *Acc. Chem. Res.* **1986**, *19*, 406.



make these complexes quite reactive toward unsaturated organic molecules or other metal complexes.^{2,3} Recent work from our lab^{2,4} and the group of Carty^{3f,g,i} has shown that this is indeed the case for several complexes exhibiting trigonal-phosphinidene bridges of the types **C** and **D**, but apparently the reactivity of binuclear complexes having bent (or pyramidal) phosphinidene bridges (**E** in Chart 1) toward organic molecules has not been explored to date, with the exception of the transient species $[\text{Fe}_2\{\mu\text{-P}(\text{N}^i\text{Pr}_2)\}_2(\text{CO})_6]$.⁵ Recently we developed a high-yield route to the diiron compounds $[\text{Fe}_2\text{Cp}_2(\mu\text{-PR})(\mu\text{-CO})(\text{CO})_2]$ ($\text{Cp} = \eta^5\text{-C}_5\text{H}_5$; $\text{R} = \text{Cy}$ (**1a**), Ph (**1b**), Chart 2), these exhibiting a quite nucleophilic bent-bridging phosphinidene ligand.⁶ A preliminary study revealed that the cyclohexylphosphinidene complex **1a** reacted with 1-alkynes and some unsaturated N-containing molecules such as trimethylsilyldiazomethane and benzyl azide to give products involving novel transformations not observed in comparable reactions of complexes having bent-terminal

(2) Amor, I.; García, M. E.; Ruiz, M. A.; Sáez, D.; Hamidov, H.; Jeffery, J. C. *Organometallics* **2006**, *25*, 4857, and references therein.

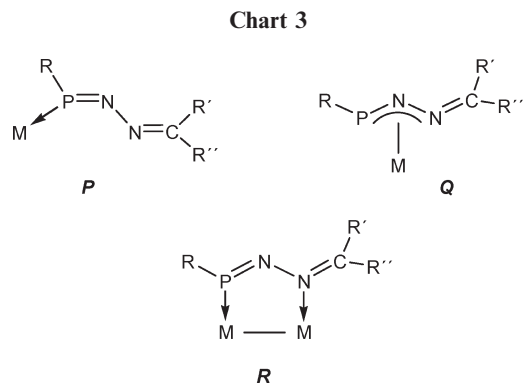
(3) For recent work on binuclear phosphinidene complexes, see: (a) Scheer, M.; Kuntz, C.; Stubenhofer, M.; Zabel, M.; Timoshkin, A. Y. *Angew. Chem., Int. Ed.* **2010**, *49*, 188. (b) Stubenhofer, M.; Kuntz, C.; Balázs, G.; Zabel, M.; Scheer, M. *Chem. Commun.* **2009**, 1745. (c) Scheer, M.; Himmel, D.; Kuntz, C.; Zhan, S.; Leiner, E. *Chem. Eur. J.* **2008**, *14*, 9020. (d) Cui, P.; Chen, Y.; Xu, X.; Sun, J. *Chem. Commun.* **2008**, 5547. (e) Masuda, J. D.; Jantunen, K. C.; Ozerov, O. V.; Noonan, J. T.; Gates, D. P.; Scott, B. L.; Kiplinger, J. L. *J. Am. Chem. Soc.* **2008**, *130*, 2408. (f) Graham, T. W.; Udachin, K. A.; Carty, A. J. *Inorg. Chim. Acta* **2007**, *360*, 1376. (g) Graham, T. W.; Udachin, K. A.; Carty, A. J. *Chem. Commun.* **2006**, 2699. (h) Bai, G.; Pingrong, W.; Das, A. K.; Stephan, D. W. *Dalton Trans.* **2006**, 1141. (i) Graham, T. W.; Udachin, K. A.; Carty, A. J. *Chem. Commun.* **2005**, 4441. (j) Shaver, M. P.; Fryzuk, M. D. *Organometallics* **2005**, *24*, 1419. (k) Driess, M.; Aust, J.; Merz, K. *Eur. J. Chem.* **2005**, 866. (l) Scheer, M.; Vogel, U.; Becker, U.; Balázs, G.; Scheer, P.; Hönle, W.; Becker, M.; Jansen, M. *Eur. J. Chem.* **2005**, 135. (m) Sanchez-Nieves, J.; Sterenberg, B. T.; Udachin, K. A.; Carty, A. J. *Can. J. Chem.* **2004**, *82*, 1507. (n) Termaten, A. T.; Nijbacker, T.; Ehlers, A. W.; Schakel, M.; Lutz, M.; Spek, A. L.; McKee, M. L.; Lammertsma, K. *Chem. Eur. J.* **2004**, *10*, 4063. (o) Sanchez-Nieves, J.; Sterenberg, B. T.; Udachin, K. A.; Carty, A. J. *Inorg. Chim. Acta* **2003**, *350*, 486. (p) Blaurock, S.; Hey-Hawkins, E. *Eur. J. Inorg. Chem.* **2002**, 2975.

(4) (a) García, M. E.; Riera, V.; Ruiz, M. A.; Sáez, D.; Vaissermann, J.; Jeffery, J. C. *J. Am. Chem. Soc.* **2002**, *124*, 14304. (b) Amor, I.; García-Vivó, D.; García, M. E.; Ruiz, M. A.; Sáez, D.; Hamidov, H.; Jeffery, J. C. *Organometallics* **2007**, *26*, 466. (c) Alvarez, M. A.; Amor, I.; García, M. E.; García-Vivó, D.; Ruiz, M. A. *Inorg. Chem.* **2007**, *46*, 6230. (d) Alvarez, M. A.; Amor, I.; García, M. E.; Ruiz, M. A. *Inorg. Chem.* **2008**, *47*, 7963.

(5) (a) King, R. B. *J. Organomet. Chem.* **1998**, *557*, 29. (b) King, R. B.; Bitterwolf, T. E. *Coord. Chem. Rev.* **2000**, *206–207*, 563.

(6) Alvarez, C. M.; Alvarez, M. A.; García, M. E.; González, R.; Ruiz, M. A.; Hamidov, H.; Jeffery, J. C. *Organometallics* **2005**, *24*, 5503.

(7) Alvarez, M. A.; García, M. E.; González, R.; Ruiz, M. A. *Organometallics* **2008**, *27*, 1037.



(**A**, **B**) or trigonal-bridging (**C**, **D**) phosphinidene ligands.⁷ In this paper we report a complete study on the reactions of the phosphinidene complex **1a** toward different diazoalkanes $\text{N}_2\text{CR}'\text{R}''$ ($\text{R}' = \text{H}$, $\text{R}'' = \text{H}$, CO_2Et , SiMe_3 ; $\text{R}' = \text{R}'' = \text{Ph}$) and the rearrangements induced by the decarbonylation of the products initially formed in these reactions. In order to examine the influence of the substituent at the phosphorus atom, we have also studied some reactions using the phenylphosphinidene complex **1b**, as well as the supermesitylphosphinidene complex $[\text{Fe}_2\text{Cp}_2(\mu\text{-PMes}^*)(\mu\text{-CO})(\text{CO})_2]$ (**1c**) ($\text{Mes}^* = 2,4,6\text{-C}_6\text{H}_2\text{Bu}_3$), the latter being a sterically congested molecule recently reported by us.⁸

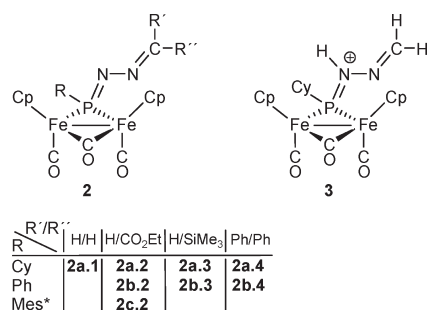
It is well known that phosphines (PR_3) react easily with diazoalkanes to give the corresponding adducts $\text{R}_3\text{PN}_2\text{-CR}'\text{R}''$,⁹ and it might be then anticipated that bent-terminal and bent-bridging phosphinidene complexes might analogously react with diazoalkanes to give initially coordinated phosphadiazadiene (or phosphazine) $\text{RPN}_2\text{CR}'\text{R}''$ ligands, a type of molecule unknown in the free state, and perhaps phosphalkene ligands ($\text{RP}=\text{CR}'\text{R}''$), if spontaneous denitrogenation could take place afterward. Surprisingly, however, the reactions of phosphinidene complexes toward diazoalkanes have been explored only recently and even so to a limited extent. In particular, it has been shown on one hand that the mononuclear electrophilic complexes $[\text{ML}(\text{CO})_x(\text{PN}^i\text{Pr}_2)]^+$ ($\text{M} = \text{Fe}, \text{Cr}, \text{Mo}, \text{W}$; $\text{L} = \text{Cp}, \text{Cp}^*$; $x = 2, 3$) (type **A**) react with N_2CPh_2 to give *P*- or *P,N,N*-bound phosphadiazadiene derivatives depending on the metal (modes **P** and **Q** in Chart 3), while the iron complex also reacts with $\text{N}_2\text{CHSiMe}_3$ to give the corresponding phosphalkene, thus implying a fast denitrogenation reaction in that case.¹⁰ On the other hand, the binuclear complex $[\text{Mn}_2(\mu\text{-PN}^i\text{Pr}_2)(\text{CO})_8]$, having a trigonal-phosphinidene bridge of type **C**, has been shown to react with N_2CPh_2 to give the *P:N*-bridged derivative $[\text{Mn}_2(\mu\text{-}^i\text{Pr}_2\text{NPN}_2\text{CPh}_2)(\text{CO})_8]$, thus providing a third coordination mode for the phosphadiazadiene ligand (**R** in Chart 3).³¹ No other reactions of phosphinidene complexes with diazoalkanes appear to have been investigated previously. Therefore, the reactions of complexes **1a–c** reported in this work constitute the first study on this matter involving bent-bridging phosphinidene complexes (type **E** in Chart 1). As it will be seen below, this has allowed the isolation of complexes having phosphadiazadiene ligands exhibiting

(8) Alvarez, M. A.; García, M. E.; González, R.; Ramos, A.; Ruiz, M. A. *Organometallics* **2010**, *29*, 1875.

(9) (a) Bethell, D.; Bourne, R.; Kasran, M. *J. Chem. Soc., Perkin Trans. 2* **1994**, 2081, and references therein. (b) Khaskin, B. A.; Molodova, O. D.; Torgasheva, N. A. *Russ. Chem. Rev.* **1992**, *61*, 306.

(10) Graham, T. W.; Udachin, K. A.; Carty, A. J. *Chem. Commun.* **2005**, 5890.

Chart 4



three new coordination modes, as well as the observation of unusual migratory processes in these ligands, resulting in novel aminophosphide-iminoacyl derivatives.

Results and Discussion

Reactions of Compounds 1 with Diazoalkanes. Structural Characterization of *P:P*-Bridged Phosphadiazadiene Derivatives. The cyclohexylphosphinidene complex **1a** reacts rapidly (in a few minutes) with the diazoalkanes N₂CR'R'' (R' = H, R'' = H, CO₂Et, R' = R'' = Ph) in dichloromethane solution at room temperature or below to give the corresponding *P:P*-bridged phosphadiazadiene derivatives [Fe₂Cp₂(μ-CyPN₂CR'R'')(μ-CO)(CO)₂] (**2a.1** to **2a.4**) with good yield (Chart 4). The presence of electron-withdrawing groups in the diazoalkane seems to be beneficial for this reaction to proceed at a high rate, since that with trimethylsilyldiazomethane requires ca. 16 h for completion under comparable conditions, even when the corresponding reaction product (**2a.3**) has the same structure as the other products. A similar reaction takes place with the phenylphosphinidene complex **1b** to give the corresponding derivatives [Fe₂Cp₂(μ-PhPN₂CR'R'')(μ-CO)(CO)₂] (**2a.2** to **2a.4**), although the reaction now occurs at a higher rate (cf. 2 h for completion in the case of N₂CHSiMe₃). The steric effects seem to have little influence in this reaction, since the reaction of ethyldiazoacetate with the supermesitylphosphinidene complex **1c** still proceeds rapidly at room temperature to give the corresponding phosphadiazadiene derivative [Fe₂Cp₂(μ-Mes*PN₂CH(CO₂Et))(μ-CO)(CO)₂] (**2c.2**). All these products could be isolated as dark green solids of medium to high sensitivity to air.

The structure of the diazomethane derivative **2a.1** was established by an X-ray study (Figure 1 and Table 1) and can be related to the structure of the phosphinidene complexes **1b,c**, and even more closely to that of the oxophosphinidene derivative [Fe₂Cp₂{μ-P(O)Cy}(μ-CO)(CO)₂].^{6,8} The molecule is built up from two cyclopentadienylcarbonyliron fragments placed in a *cisoid* relative arrangement, these being bridged by a carbonyl and by a phosphadiazadiene ligand bound to the iron centers through its P atom, with the cyclohexyl group pointing away from the cyclopentadienyl ligands, as found in the phosphinidene precursor. The environment around the iron atoms is pseudooctahedral, and the intermetallic distance of 2.6198(6) Å is comparable to those measured in the mentioned compounds (cf. 2.601(2) Å for the oxophosphinidene complex) and consistent with the single Fe–Fe bond proposed for all these molecules according to the EAN rule. The major perturbation on the metal environment derived from the binding of the diazoalkane molecule to the phosphorus atom concerns the Fe–P bond lengths, which are reduced from ca. 2.26 Å in **1b** to ca. 2.22 Å in **2a.1**, as also

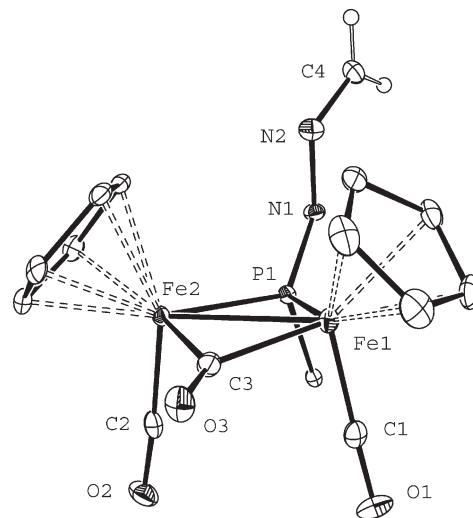


Figure 1. ORTEP diagram (30% probability) of compound **2a.1**, with the Cy ring (except the C¹ atom) and H atoms (except those bound to C⁴) omitted for clarity.

Table 1. Selected Bond Lengths (Å) and Angles (deg) for Compound **2a.1**

Fe(1)–Fe(2)	2.6198(6)	Fe(1)–P(1)–Fe(2)	72.06(2)
Fe(1)–P(1)	2.2180(8)	Fe(1)–C(3)–Fe(2)	85.2(1)
Fe(2)–P(1)	2.2359(8)	Fe(1)–Fe(2)–C(2)	100.2(1)
Fe(1)–C(3)	1.939(3)	Fe(2)–Fe(1)–C(1)	98.8(1)
Fe(2)–C(3)	1.931(3)	P(1)–Fe(1)–C(1)	90.1(1)
Fe(1)–C(1)	1.749(3)	P(1)–Fe(2)–C(2)	91.3(1)
Fe(2)–C(2)	1.750(3)	C(3)–Fe(1)–C(1)	89.3(1)
P(1)–N(1)	1.612(2)	C(3)–Fe(2)–C(2)	90.0(1)
N(1)–N(2)	1.403(3)	P(1)–Fe(1)–C(3)	100.3(1)
N(2)–C(4)	1.278(4)	Fe(1)–P(1)–N(1)	124.5(1)
		P(1)–N(1)–N(2)	117.5(2)
		N(1)–N(2)–C(4)	116.1(3)

observed in the formation of the mentioned oxophosphinidene complex.⁶ Yet all these values are within the range of single-bond lengths. To our knowledge, compound **2a.1** represents the first example of a complex displaying a bridging phosphadiazadiene ligand bound to the metal centers exclusively through the phosphorus atoms. This expectedly leads to Fe–P distances longer than in the terminal mode (**P** in Chart 3, cf. 2.1691(4) Å in [FeCp(CO)₂(Pr₂NPN₂CPh₂)]⁺).¹⁰ Yet, the P–N, N–N, and N–C distances of ca. 1.60, 1.40, and 1.30 Å, respectively, are comparable in both complexes. Taking into account the reference values for the respective single and double bonds, as well as the effect of hybridization,¹¹ these distances can be taken as indicative of the presence of essentially double, single, and double bonds, respectively, which is also in agreement with the values of the P–N–N and N–N–C angles, close to 120°. Finally, we should remark that the PNNC skeleton adopts a *transoid*, almost planar configuration (torsion angle 166°) perpendicular to the intermetallic bond, perhaps just to minimize the repulsive interactions with the cyclopentadienyl ligands.

Spectroscopic data in solution for the eight compounds of type **2** prepared are similar to each other (Table 2 and Experimental Section), thus indicating that they all share the same structure, comparable to that of **2a.1** in the crystal. In particular, their IR spectra exhibit a low-frequency band

(11) (a) Huheey, J. E.; Keiter, E. A.; Keiter, R. L. *Inorganic Chemistry: Principles of Structure and Reactivity*, 4th ed.; HarperCollins College Publishers: New York, 1993. (b) Allen, F. H.; Kennard, O.; Watson, D. G.; Brammer, L.; Orpen, G.; Taylor, R. *J. Chem. Soc., Perkin Trans. 2* **1987**, S1.

Table 2. Selected IR and $^{31}\text{P}\{^1\text{H}\}$ NMR Data for New Compounds

compound	$\nu(\text{CO})^a$	δ_{P}^b	$\delta_{\text{C}}(J_{\text{CP}})^c$
$[\text{Fe}_2\text{Cp}_2(\mu\text{-CyPN}_2\text{CH}_2)(\mu\text{-CO})(\text{CO})_2]$ (2a.1)	1980 (vs), 1946 (w), 1780 (m)	307.6	133.7 (51)
$[\text{Fe}_2\text{Cp}_2\{\mu\text{-CyPN}_2\text{CH}(\text{CO}_2\text{Et})\}(\mu\text{-CO})(\text{CO})_2]$ (2a.2)	1988 (vs), 1955 (w), 1791 (m), 1684 (m)	332.4 ^d	130.0 (55) ^d
$[\text{Fe}_2\text{Cp}_2\{\mu\text{-CyPN}_2\text{CH}(\text{SiMe}_3)\}(\mu\text{-CO})(\text{CO})_2]$ (2a.3)	1980 (vs), 1947 (w), 1782 (m)	304.8	
$[\text{Fe}_2\text{Cp}_2(\mu\text{-CyPN}_2\text{CPh}_2)(\mu\text{-CO})(\text{CO})_2]$ (2a.4)	1980 (vs), 1947 (w), 1781 (m)	301.0	
$[\text{Fe}_2\text{Cp}_2\{\mu\text{-PhPN}_2\text{CH}(\text{CO}_2\text{Et})\}(\mu\text{-CO})(\text{CO})_2]$ (2b.2)	1998 (vs), 1965 (w), 1797 (m), 1687 (m)	315.0 ^d	
$[\text{Fe}_2\text{Cp}_2\{\mu\text{-PhPN}_2\text{CH}(\text{SiMe}_3)\}(\mu\text{-CO})(\text{CO})_2]$ (2b.3)	1991 (vs), 1955 (w), 1785 (m)	292.7	
$[\text{Fe}_2\text{Cp}_2(\mu\text{-PhPN}_2\text{CPh}_2)(\mu\text{-CO})(\text{CO})_2]$ (2b.4)	1990 (vs), 1956 (w), 1786 (m)	289.0	
$[\text{Fe}_2\text{Cp}_2\{\mu\text{-Mes}^*\text{PN}_2\text{CH}(\text{CO}_2\text{Et})\}(\mu\text{-CO})(\text{CO})_2]$ (2c.2)	1998 (vs), 1968 (w), 1782 (m), 1678 (m)	318.3	126.3 (61)
$[\text{Fe}_2\text{Cp}_2(\mu\text{-CyPNHNCH}_2)(\mu\text{-CO})(\text{CO})_2](\text{BF}_4)$ (3)	2012 (vs), 1982 (w), 1825 (m)	313.7	
$[\text{Fe}_2\text{Cp}_2(\mu\text{-CyPN}_2\text{CH}_2)(\mu\text{-CO})_2]$ (4)	1780 (w), 1745 (vs)	204.8 ^d	
<i>cis</i> - $[\text{Fe}_2\text{Cp}_2(\mu\text{-}\kappa^1\text{-}\eta^2\text{-CyPCH}_2)(\mu\text{-CO})(\text{CO})]$ (<i>cis</i> - 5)	1939 (vs), 1860 (w, br) ^e	208.2	20.3 (4)
<i>trans</i> - 5	1895 (vs) ^{e,f}	193.0	
$[\text{Fe}_2\text{Cp}_2\{\mu\text{-CyPN}_2\text{CH}(\text{CO}_2\text{Et})\}(\mu\text{-CO})(\text{CO})]$ (6)	1936 (vs), 1783 (s), 1683 (m) ^g		
<i>cis</i> - $[\text{Fe}_2\text{Cp}_2\{\mu\text{-CyPNHNC}(\text{CO}_2\text{Et})\}(\mu\text{-CO})(\text{CO})]$ (<i>cis</i> - 7e)	1967 (vs), 1788 (s), 1697 (m)	334.8	
<i>trans</i> - 7e	1942 (vs), 1788 (s), 1697 (m)	326.0	191.9 (11)
<i>cis</i> - $[\text{Fe}_2\text{Cp}_2\{\mu\text{-CyPN}(\text{SiMe}_3)\text{NCH}\}(\mu\text{-CO})(\text{CO})]$ (<i>cis</i> - 7f)	1953 (vs), 1782 (s) ^g	352.7	182.5 (11)
<i>trans</i> - 7f	1934 (vs) ^{g,f}	344.6	191.8 (11)
<i>cis</i> - $[\text{Fe}_2\text{Cp}_2(\mu\text{-CyPNHNCH})(\mu\text{-CO})(\text{CO})]$ (<i>cis</i> - 7g)	1960 (vs), 1771 (s)	334.5 ^h	188.9 (5)
<i>trans</i> - 7g	1934 (vs) ^f	315.4 ^g	
<i>cis</i> - $[\text{Fe}_2\text{Cp}_2(\mu\text{-CyPNHNHCH})(\mu\text{-CO})(\text{CO})](\text{BF}_4)$ (<i>cis</i> - 8j)	1990 (vs), 1803 (s)	320.6	220.4 (16)
<i>trans</i> - 8j	1966 (vs) ^f	313.6	
<i>cis</i> - $[\text{Fe}_2\text{Cp}_2(\mu\text{-CyPNHNMeCH})(\mu\text{-CO})(\text{CO})](\text{I})$ (<i>cis</i> - 8k)	1984 (vs), 1798 (s)	322.8	222.2 (18)
<i>trans</i> - 8k	1960 (vs) ^f	315.0	
$[\text{Fe}_2\text{Cp}_2(\mu\text{-Mes}^*\text{PN}_2\text{CH}_2)(\mu\text{-CO})_2]$ (9)	1794 (w), 1764 (vs), 1710 (w) ⁱ	328.6	133.9 (27)

^a Recorded in dichloromethane solution, C–O stretching bands ($\nu(\text{CO})$) in cm^{-1} ; in complexes with CO_2Et groups, the band at the lowest frequency is due in each case to the corresponding C=O stretch. ^b Recorded in CD_2Cl_2 solutions at 290 K and 121.50 MHz; δ in ppm relative to external 85% aqueous H_3PO_4 . ^c ^{13}C NMR resonance for the methylenic carbon of the former diazoalkane molecule, recorded in CD_2Cl_2 solutions at 290 K and 75.48 MHz; δ in ppm relative to internal TMS and J_{CP} in Hz. ^d In CDCl_3 solution. ^e In tetrahydrofuran solution. ^f The band at lower frequency could not be identified in the spectrum, it being obscured by the lower frequency band of the major isomer. ^g In toluene solution. ^h Recorded at 162.00 MHz (^{31}P) or 100.62 MHz (^{13}C) and 253 K. ⁱ Recorded in petroleum ether solution.

at ca. 1780 cm^{-1} corresponding to the bridging carbonyl, and two high-frequency bands at ca. 1980 and 1950 cm^{-1} , with relative intensities (strong and weak, in order of decreasing frequencies) characteristic of $\text{M}_2(\text{CO})_2$ oscillators with almost parallel carbonyl ligands.¹² Compounds **2** exhibit ^{31}P NMR resonances in the range 290–330 ppm, a bit more shielded than the related oxophosphinidene complexes (315–345 ppm),^{6,8} with the ethyldiazoacetate derivatives giving the most deshielded resonances. In any case, these values are comparable or somewhat higher than that reported for the terminal phosphadiazadiene complex $[\text{FeCp}(\text{CO})_2(\text{Pr}_2\text{NPN}_2\text{CPh}_2)]^+$ (291 ppm),¹⁰ which is somewhat unexpected since, for instance, bridging phosphines ($\mu\text{-PR}_3$) give rise to ^{31}P resonances more shielded than comparable terminal ligands.¹³ This suggests that the ^{31}P shielding in the phosphadiazadiene complexes is most likely determined by the presence of substantial multiplicity in the P–N bond. The uncoordinated methylenic groups in compounds **2** give rise to ^1H NMR resonances at ca. 7.5 ppm, as expected, and to ^{13}C resonances at ca. 130 ppm, a characteristic shift for sp^2 C atoms. The latter resonances exhibit large three-bond couplings to phosphorus (50–60 Hz), comparable to those measured for the phosphine adducts of diazoalkanes (e.g., 50 Hz for $\text{Ph}_3\text{PN}_2\text{CPh}(\text{CN})$).¹⁴ In the case of the diazomethane derivative **2a.1**, the coupling between the methylenic hydrogens (15 Hz) is much higher than expected for a geminal coupling at a conventional sp^2 carbon atom (0–3 Hz),

although we note that, for instance, the geminal couplings in allenes are substantially higher (ca. 9 Hz).¹⁵ All the above data might be suggestive of the presence of some delocalization of the π bonding along the PNNC chain, which itself would not be inconsistent with the geometrical data found in the solid state for **2a.1**.

Solid-State and Solution Structure of the Aminophosphide Derivative 3. The presence of lone electron pairs at the N atoms in complexes **2** should allow further functionalization of these molecules through the reactions with suitable electrophiles. Indeed this seems to be the case since, for instance, the diazomethane derivative **2a.1** is instantaneously protonated by $\text{HBF}_4\cdot\text{OEt}_2$ in dichloromethane solution to give the corresponding salt $[\text{Fe}_2\text{Cp}_2(\mu\text{-CyPNHNCH}_2)(\mu\text{-CO})(\text{CO})_2](\text{BF}_4)$ (**3**) in quantitative yield (Chart 4). A single-crystal X-ray study confirmed the incorporation of the added proton to the nitrogen atom bound to phosphorus (Figure 2 and Table 3), which otherwise caused little perturbation to the overall structure of the complex. The most significant differences found in **3** are a slight contraction (by ca. 0.04 Å) of the Fe–P lengths and perhaps a more significant elongation of the P–N distance (to 1.669(2) Å), now approaching the single-bond figures. In contrast, the N–N and N–C lengths in the ligand chain remain unperturbed after protonation. This can be explained by considering that the phosphinidene–diazomethane interaction present in compound **2** must be biphilic in nature, as found for the phosphine/diazomethane adducts,^{9a} then having σ (P to N) and π (N to P) components. Because of the positive charge developed at the P-bound nitrogen upon protonation, the π contribution would be greatly diminished, leaving an essentially single P–N bond. As a result, the new P-donor group might be better described now as an aminophosphide ligand. The degree of pyramidalization of the protonated nitrogen, however, seems to be small, as indicated by the sum of bond

(12) Braterman, P. S. *Metal Carbonyl Spectra*; Academic Press: London, U.K., 1975.

(13) (a) Pechmann, T.; Brandst, C. D.; Werner, H. *Chem. Eur. J.* **2004**, *10*, 728. (b) Werner, H. *Angew. Chem., Int. Ed.* **2004**, *43*, 938.

(14) Molina, P.; Lopez-Leonardo, C.; Llamas-Botia, J.; Foces-Foces, C.; Fernández-Castaño, C. *Tetrahedron* **1996**, *52*, 9629.

(15) Pretsch, E.; Bühlmann, P.; Badertscher, M. *Structural Determination of Organic Compounds*, 4th ed.; Springer: Heidelberg, Germany, 2009.

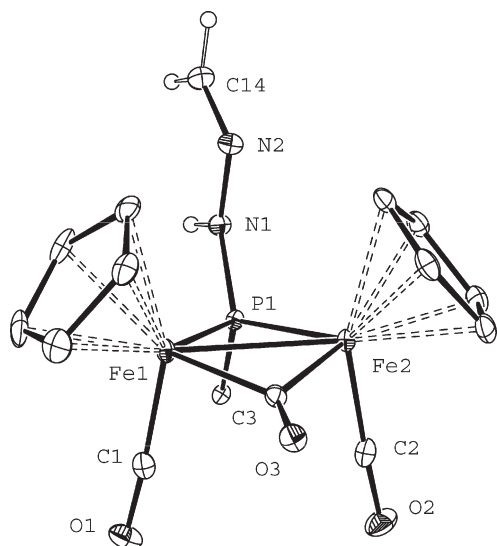


Figure 2. ORTEP diagram (30% probability) of the cation in compound **3**, with the Cy ring (except the C¹ atom) and H atoms (except those bound to N and C⁴) omitted for clarity.

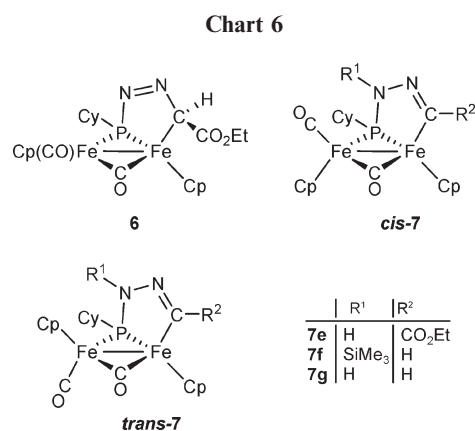
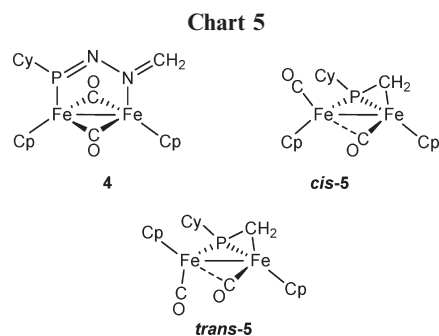
Table 3. Selected Bond Lengths (Å) and Angles (deg) for Compound 3

Fe(1)–Fe(2)	2.6126(5)	Fe(1)–P(1)–Fe(2)	73.57(2)
Fe(1)–P(1)	2.1855(6)	Fe(1)–C(3)–Fe(2)	84.6(1)
Fe(2)–P(1)	2.1772(7)	Fe(1)–Fe(2)–C(2)	100.2(1)
Fe(1)–C(3)	1.935(2)	Fe(2)–Fe(1)–C(1)	100.7(1)
Fe(2)–C(3)	1.948(2)	P(1)–Fe(1)–C(1)	90.9(1)
Fe(1)–C(1)	1.763(2)	P(1)–Fe(2)–C(2)	92.0(1)
Fe(2)–C(2)	1.766(2)	C(3)–Fe(1)–C(1)	90.5(1)
P(1)–N(1)	1.669(2)	C(3)–Fe(2)–C(2)	88.9(1)
N(1)–N(2)	1.388(2)	P(1)–Fe(1)–C(3)	99.3(1)
N(2)–C(14)	1.269(3)	Fe(1)–P(1)–N(1)	121.1(1)
N(1)–H(2)	0.81(2)	P(1)–N(1)–N(2)	119.9(2)
		N(1)–N(2)–C(14)	116.3(2)

angles around nitrogen (356.5°). This figure, however, must be taken with caution, due to the low precision of the angles involving the H atom and the involvement of the latter in a strong hydrogen-bond interaction with the BF₄[−] anion (H⋯F ca. 2.18 Å).

Spectroscopic data in solution for **3** are fully consistent with the structure in the crystal just discussed. In particular, the pattern of the C–O stretching bands is identical to that in the precursor **2a.1**, with average C–O stretching frequencies some 40 cm^{−1} higher, as expected. In contrast, the ³¹P chemical shift of **3** is comparable to that of its precursor in spite of the substantial modifications occurring at the phosphorus site, an observation that can be explained only if different effects (e.g., charge and P–N bond order) counterbalance their respective influences.

Decarbonylation Reactions of Phosphadiazadiene Complexes. Since the *P:P*-bound bridging ligands in compounds **2** still have several potentially donor centers, such as the nitrogen atoms or even the N=C(R')R'' bond, it was of interest to examine whether these donor centers would be involved in bonding with the dimetal site when creating a coordination vacant in the latter by removal of a CO molecule. A second point of interest was to check whether denitrogenation could also be induced in these complexes, to give phosphalkene derivatives. With this purpose, we studied the behavior of compounds **2** under conditions of thermal and photochemical activation.



When heating toluene solutions of compounds **2**, a progressive decomposition takes place in all cases to give the dimer [Fe₂Cp₂(CO)₄] as the only organometallic product, the transformations being typically completed in ca. 1–2 h at 363 K. A similar result was obtained when irradiating with visible–UV light toluene solutions of the phenyl compounds **2b.2** to **2b.4**. In contrast, relatively selective decarbonylations could be induced photochemically on the cyclohexyl (except **2a.4**) and supermesityl compounds. The reaction products, however, were strongly dependent on the substituents at either the P atom or the methylenic carbon. Thus the diazomethane derivative **2a.1** yielded a mixture of the *P:N*-bound phosphadiazadiene complex [Fe₂Cp₂(μ-CyPN₂CH₂)(μ-CO)₂] (**4**) and the phosphalkene derivative [Fe₂Cp₂(μ-CyPCH₂)(μ-CO)(CO)] (**5**) (Chart 5). In contrast, the ethyldiazoacetate derivative gave the paramagnetic complex [Fe₂Cp₂{μ-CyPN₂CH(CO₂Et)}(μ-CO)(CO)] (**6**), possibly containing a *μ-P:P,C*-phosphadiazadiene ligand (Chart 6). Finally, the trimethylsilyldiazomethane derivative instead gave selectively the aminophosphide-iminoacyl complex [Fe₂Cp₂{μ-CyPN(SiMe₃)NCH}(μ-CO)(CO)] (**7f**) (Chart 6). As for the influence of the substituent at phosphorus on these reactions, we note that the decarbonylation of the ethyldiazoacetate derivative **2c.2** gave the complex [Fe₂Cp₂{μ-Mes*PN₂CH(CO₂Et)}(μ-CO)₂] (**9**), containing a *μ-P:N*-phosphadiazadiene ligand bound to the dimetal center through the P-bound nitrogen atom (Chart 8).

Solution Structure of the Diazomethane Derivatives 4 and 5. Although the complexes **4** and **5** differ in a molecule of nitrogen, they were always obtained by us in a similar ratio (ca. 3:1). Modifications in solvent (toluene vs tetrahydrofuran), temperature (288 vs 263 K), or reaction time caused no significant changes in this ratio. Thus, it is concluded that compound **5** is not formed from **4**, but through an independent reaction pathway.

The presence of two nitrogen atoms in **4** is unambiguously established by the microanalytical data. In addition, its IR spectrum exhibits two C–O stretching bands in the region of the bridging ligands, with relative intensities characteristic of $M_2(\mu\text{-CO})_2$ oscillators with almost antiparallel CO ligands,¹² as usually found for diphosphine-bridged (L_2) complexes of the type $[\text{Fe}_2\text{Cp}_2(\mu\text{-CO})_2(\mu\text{-L}_2)]$. Actually, the ³¹P chemical shift of the bridging ligand in **4** (204.8 ppm) is not much higher than those of the mentioned diiron complexes when the diphosphine ligand has P–O or P–N bonds, such as $(\text{EtO})_2\text{POP}(\text{OEt})_2$ (179.1 ppm)¹⁶ or $\text{R}_2\text{PN}(\text{Me})\text{PNR}_2$ (160–180 ppm).¹⁷ Thus we propose that the phosphadiazadiene ligand in **4** is bridging the dimetal center through the phosphorus and C-bound nitrogen atoms (mode **R** in Chart 3), as crystallographically determined for the dimanganese complex $[\text{Mn}_2(\mu\text{-}^i\text{Pr}_2\text{NPN}_2\text{CPh}_2)(\text{CO})_8]$.³¹ The latter complex, however, exhibits a more deshielded ³¹P resonance (δ 285 ppm), a difference for which we cannot give a satisfactory explanation at the moment. Finally, the ¹H NMR spectrum of **4** displays inequivalent cyclopentadienyl and methylenic resonances, in agreement with the proposed structure. Yet, the latter resonances (δ ca. 4 ppm) are more shielded than expected for an uncoordinated $\text{N}=\text{CH}_2$ group. Unfortunately, we could not obtain a satisfactory ¹³C NMR spectrum of **4** to gain further structural information on this molecule, due to its low solubility in most common solvents.

The microanalytical data for **5** clearly reveal the absence of nitrogen in this molecule, while the NMR data denote the presence of *cis* and *trans* isomers in solution (Chart 5), with their relative ratio (ca. 10:1) being unaffected by changes in solvent or temperature. The IR spectrum of **5** in petroleum ether solution displays two sharp C–O stretching bands of strong and weak intensities at 1955 and 1906 cm^{-1} and a broad weak band at 1865 cm^{-1} . The first and third band are then assigned to the major isomer, and the low frequency and broadness of the weaker band is suggestive of the presence of a semibridging carbonyl in this isomer, in agreement with the ¹³C NMR data to be discussed later on. The minor isomer possibly displays a similar pattern, although only the sharp band at higher frequency can be identified in the spectrum of the mixture. By comparison with the IR data of the *cis* and *trans* isomers of the structurally related phosphide-acyl complex $[\text{Fe}_2\text{Cp}_2\{\mu\text{-}\kappa^1\text{:}\kappa^1\text{:}\eta^1\text{-CypCHC}(p\text{-tol})\text{C}(\text{O})\}(\mu\text{-CO})(\text{CO})]$,⁷ we can identify the isomer giving rise to the more energetic terminal C–O stretch as the *cis* isomer. As it will be seen later, *cis* and *trans* isomers are also observed for complexes **7** and **8**, and they also seem to follow the same spectroscopic trend, which, incidentally, is the same trend observed for the *cis* and *trans* isomers of the phosphine complexes of general formula $[\text{Fe}_2\text{Cp}_2(\mu\text{-CO})_2(\text{CO})(\text{PR}_3)]$.¹⁸

The presence of a phosphalkene ligand bridging the dimetal center in an $\mu\text{-}\eta^1\text{:}\eta^2$ -alkenyl-like fashion is denoted in the major isomer by the presence of quite shielded resonances for the methylene group in the corresponding

¹³C and ¹H NMR spectra, in positions comparable to those of the structurally characterized dicobalt complex $[\text{Co}_2(\text{CO})_4(\mu\text{-}^i\text{Pr}_2\text{NPCH}_2)(\mu\text{-dppm})]$ ³¹ and other phosphalkene-bridged complexes.¹⁹ Interestingly, the dicobalt complex was directly obtained in the reaction of diazomethane with the trigonal-phosphinidene complex $[\text{Co}_2(\text{CO})_4(\mu\text{-PN}^i\text{Pr}_2)(\mu\text{-dppm})]$ (dppm = $\text{Ph}_2\text{PCH}_2\text{PPh}_2$). The phosphorus resonances of both isomers of **5** (δ_{P} 208.2 and 193.0 ppm) also appear in a position comparable to that of the mentioned dicobalt complex (δ_{P} 247 ppm). Finally, the presence of semibridging and terminal carbonyls in the major isomer of **5** is substantiated by the appearance of quite differently deshielded ¹³C resonances for these ligands, at 237.8 and 219.3 ppm, respectively, with the latter being within the typical range of terminal ligands (210–220 ppm) and the other being significantly shifted toward the usual region of bridging carbonyls (255–280 ppm).

Solution Structure of the Paramagnetic Complex 6. The magnetic susceptibility of **6** was measured in CD_2Cl_2 solution by the NMR method developed by Evans,²⁰ yielding an effective magnetic moment of 2.75 μ_{B} , which is very close to the spin-only value for a complex with two unpaired electrons (2.83 μ_{B}). On the other hand, its IR spectrum displays C–O stretching bands indicative of the presence of one terminal and one bridging carbonyl. Actually, these bands are comparable to those of its diamagnetic derivative *trans*-**7e** (Table 2), which we have fully characterized (see below). For this reason, we propose that the phosphadiazadiene ligand in **6** displays a coordination mode comparable to that of its aminophosphide-iminoacyl derivative **7e**, with the methylenic carbon occupying the vacant position left by the carbonyl ligand being removed. As a result of the strong electronic rearrangement implied, the phosphadiazadiene ligand would then become a sort of phosphide-alkyl ligand (Chart 6), although, due to the scarce spectroscopic data available, this structural proposal must be obviously taken with great caution. Unfortunately, all our attempts to obtain good-quality crystals of **6** for an X-ray study were unsuccessful. Yet, another puzzling question is the presence of unpaired electrons in this molecule, a feature very unusual for binuclear carbonyl complexes of the transition metals, which are generally able to form strong intermetallic bonds. We trust that, for some reason, the Fe–Fe bond in **6** might be particularly weak so as to yield singlet and triplet spin states of comparable energy. For instance, the 32-electron complex $[\text{Fe}_2\text{Cp}_2^*(\mu\text{-CO})_3]$ is paramagnetic ($\mu_{\text{eff}} = 2.5 \mu_{\text{B}}$ in the solid state), in this case due to a symmetry-imposed triplet spin state,²¹ and even a more complex situation (several singlet and triplet states of comparable energies) has been recently uncovered computationally for the isoelectronic cyclobutadiene complex $[\text{Fe}_2(\eta^4\text{-C}_4\text{H}_4)_2(\mu\text{-CO})_2(\text{CO})_2]$.²²

Formation and Solid-State and Solution Structure of Compounds 7. Upon column chromatography on alumina, the paramagnetic complex **6** fully rearranges into the diamagnetic isomer $[\text{Fe}_2\text{Cp}_2\{\mu\text{-CypNHNC}(\text{CO}_2\text{Et})\}(\mu\text{-CO})(\text{CO})]$ (**7e**), which contains an aminophosphide-iminoacyl ligand formally derived from a 1,3-shift of the methylenic hydrogen up to the P-bound nitrogen atom. Since this transformation

(16) Alvarez, C. M.; Galán, B.; García, M. E.; Riera, V.; Ruiz, M. A.; Bois, C. *Organometallics* **2003**, *22*, 3039.

(17) Wang, N.; Wang, M.; Liu, T.; Li, P.; Zhang, T.; Darenbourg, M. Y.; Sun, L. *Inorg. Chem.* **2008**, *47*, 6948.

(18) (a) Haines, R. J.; du Preez, A. L. *Inorg. Chem.* **1969**, *8*, 1459. (b) Klasek, C.; Lorenz, I. P.; Schmid, S.; Beuter, G. *J. Organomet. Chem.* **1992**, *428*, 363. (c) Zhang, S.; Brown, T. L. *Organometallics* **1992**, *11*, 4166.

(19) (a) Lang, H.; Leise, M. *J. Organomet. Chem.* **1993**, *456*, C4. (b) Weber, L.; Schumann, I.; Stammel, H. G.; Neumann, B. *Organometallics* **1995**, *14*, 1626. (c) Davies, J. E.; Mays, M. J.; Raithby, P. R.; Woods, A. D. J. *Chem. Soc., Chem. Commun.* **1999**, 2455.

(20) (a) Evans, J. J. *Am. Chem. Soc.* **1960**, *82*, 5145. (b) Grant, D. H. *J. Chem. Educ.* **1995**, *72*, 39.

(21) Blaha, J. P.; Bursten, B. E.; Dewan, J. C.; Franke, R. B.; Randolph, C. L.; Wilson, B. A.; Wrighton, M. S. *J. Am. Chem. Soc.* **1985**, *107*, 4561.

(22) Wang, H.; Xie, Y.; King, R. B.; Schaefer, H. F., III. *Organometallics* **2008**, *27*, 3113.

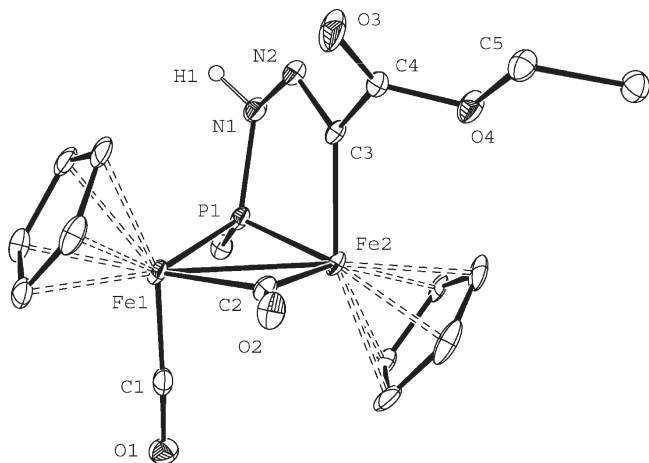


Figure 3. ORTEP diagram (30% probability) of one of the two independent molecules found in the crystal lattice of compound **7e**, with the Cy ring (except the C¹ atom) and H atoms (except H1) omitted for clarity.

could not be induced by either thermal or photochemical activation of **6**, it does not seem to be intramolecular in nature, but possibly results from a protonation/deprotonation sequence on the alumina surface. In contrast, the photochemical treatment of the trimethylsilyl compound **2a.3** gives directly the dicarbonyl [Fe₂Cp₂{μ-CyPN(SiMe₃)-NCH}(μ-CO)(CO)] (**7f**), having a related bridging ligand now derived from a 1,3-shift of the SiMe₃ group (presumably intramolecular) up to the P-bound nitrogen atom. In turn, the SiMe₃ group in **7f** is easily hydrolyzed either by addition of water (30 min upon addition of 2 equiv of H₂O to a toluene solution) or upon column chromatography on alumina (activity IV), to give almost quantitatively the corresponding derivative [Fe₂Cp₂(μ-CyPNHNCH)(μ-CO)(CO)] (**7g**).

The compounds **7e–g** exhibit in solution *cis* and *trans* isomers differing in the relative orientation of the cyclopentadienyl ligands with respect to the Fe₂P plane (Chart 6), as found for the phosphalkene complex **5**. However, the relative proportion and possibility of interconversion between isomers strongly depend on the substituents present at the PNNC chain, and no simple conclusion can be extracted from the observed ratios (see the Experimental Section).

We have now determined the crystal structure of the *trans* isomer of compound **7e** (Figure 3 and Table 4), while the structure of the *cis* isomer of compound **7f** was reported in our preliminary communication (Figure 4).⁷ Both structures are similar, except for the relative orientation of the FeCp(CO) moiety, with interatomic distances differing by less than ca. 0.03 Å from each other. Both molecules can be described as two iron cyclopentadienyl fragments connected by a single metal–metal bond (ca. 2.60 Å) and two bridging ligands: a carbonyl and an aminophosphide group. The coordination spheres around the iron atoms are completed by the terminal binding of an iminoacyl group (Fe–C ca. 1.95 Å) and a carbonyl ligand, placed in either a *trans* or *cis* relative arrangement. The better donor properties of the carbonyl ligand (compared to the iminoacyl donor) are counterbalanced by the bridging groups, placed closer to the acyl-bound iron atom (by ca. 0.06 Å in the case of phosphorus and by 0.15 Å for the carbonyl bridge). This structural effect was also observed in the related phosphide-acyl complex [Fe₂Cp₂{μ-κ¹:κ¹,η¹-CyPCHC(*p*-tol)C(O)}(μ-CO)(CO)], which also displays a comparable Fe–C(acyl)

Table 4. Selected Bond Lengths and Angles for Compound **7e**

Fe(1)–Fe(2)	2.6261(8)	Fe(1)–P(1)–Fe(2)	75.27(4)
Fe(1)–P(1)	2.186(1)	Fe(1)–C(2)–Fe(2)	84.1(2)
Fe(2)–P(1)	2.114(1)	Fe(1)–Fe(2)–C(3)	91.0(1)
Fe(1)–C(2)	2.039(4)	Fe(2)–Fe(1)–C(1)	88.9(1)
Fe(2)–C(2)	1.879(4)	P(1)–Fe(1)–C(1)	93.5(1)
Fe(1)–C(1)	1.756(5)	P(1)–Fe(2)–C(3)	79.6(1)
Fe(2)–C(3)	1.959(4)	C(2)–Fe(1)–C(1)	95.9(2)
P(1)–N(1)	1.697(4)	C(2)–Fe(2)–C(3)	89.8(2)
N(1)–N(2)	1.407(5)	P(1)–Fe(1)–C(2)	95.5(1)
N(1)–H(1)	0.87(6)	Fe(1)–P(1)–N(1)	118.2(1)
N(2)–C(3)	1.301(5)	Fe(2)–P(1)–N(1)	104.8(1)
C(3)–C(4)	1.508(6)	P(1)–N(1)–N(2)	110.8(3)
		N(1)–N(2)–C(3)	114.0(4)
		N(2)–C(3)–Fe(2)	125.6(3)

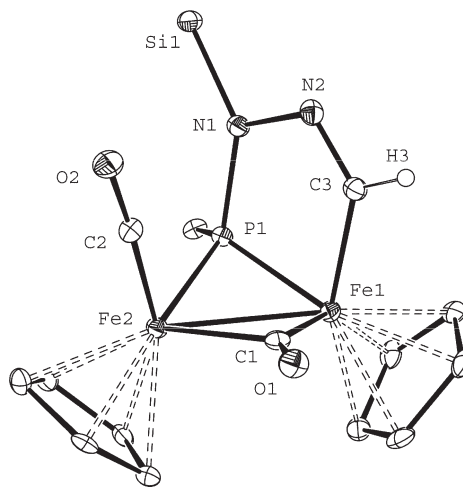
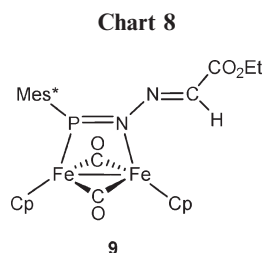
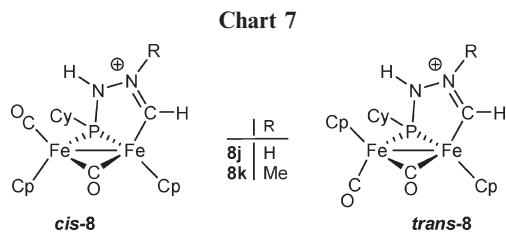


Figure 4. ORTEP diagram (30% probability) of compound **7f** (reproduced from ref 7), with the Cy ring (except the C¹ atom), Me groups, and H atoms (except H3) omitted for clarity. Selected bond lengths (Å): Fe(1)–Fe(2) = 2.5890(8), Fe(1)–P(1) = 2.149(1), Fe(2)–P(1) = 2.203(1), Fe(1)–C(1) = 1.856(4), Fe(2)–C(1) = 2.016(4), Fe(2)–C(2) = 1.743(5), Fe(1)–C(3) = 1.936(4), C(3)–N(2) = 1.284(5), N(2)–N(1) = 1.437(5), N(1)–P(1) = 1.711(4), N(1)–Si(1) = 1.760(4).

bond length of 1.967(3) Å.⁷ The interatomic distances within the PNNC chain in both complexes are similar to each other, with values of ca. 1.70 Å (P–N), 1.42 Å (N–N), and 1.29 Å (N–C), comparable to those measured in **3** and indicative of the presence of essentially single, single, and double bonds, respectively. As for the P-bound nitrogen, this bonding description should imply a pyramidal environment, which is in agreement with the angles around this atom for compound **7e**, adding up 343°. For the SiMe₃ compound **7f**, however, the environment around N(1) is trigonal, with the corresponding angles adding up 360°, possibly a steric effect minimizing the repulsions of the bulky SiMe₃ group.

The spectroscopic data in solution for compounds **7** (Table 2 and Experimental Section) are fully consistent with the solid-state structures just discussed. In particular, the IR spectra display for each isomer two C–O stretching bands at ca. 1965–1935 and 1780 cm⁻¹, corresponding respectively to the terminal and bridging carbonyls, which correlates with the appearance of resonances at ca. 212 and 268 ppm, respectively, in the corresponding ¹³C NMR spectra. The stretching frequency for the terminal carbonyl in the isomers *cis* is systematically some 20 cm⁻¹ higher than those for the corresponding isomers *trans*, as noted above. The aminophosphide ligands in all these molecules give rise to a ³¹P NMR resonance in the range 315–350 ppm, a position



reasonable for a N-substituted phosphide group (cf. 265 ppm for the mentioned phosphide-acyl complex). On the other hand, the presence of the terminally bound iminoacyl donor is revealed by the appearance in the ^{13}C NMR spectra of a resonance at ca. 190 ppm in all cases, a position substantially more shielded than that of the mentioned phosphide-acyl complex (ca. 260 ppm),⁷ as expected. The observed chemical shifts, in fact, are comparable (if we allow for the change in metal) to that of the iminoacyl ^{13}C resonance in the mononuclear phosphine-iminoacyl complex $[\text{MoCp}(\text{CO})_2\{\text{tBu}_2\text{PNHNC}(\text{CO}_2\text{Et})\}]$ (171.3 ppm).²³ Interestingly, the latter complex is formed by a route related to that leading to complexes **7**, a matter to be addressed later.

Cationic Derivatives of Compound 7g. The presence of a lone electron pair at the C-bound nitrogen atom of the bridging ligand of complexes **7** still should allow for further functionalization of these molecules through the reactions with suitable electrophiles. Indeed the unsubstituted complex **7g** reacts instantaneously with $\text{HBF}_4 \cdot \text{OEt}_2$ in dichloromethane solution to give the salt $[\text{Fe}_2\text{Cp}_2(\mu\text{-CyPNHNHCH})(\mu\text{-CO})(\text{CO})](\text{BF}_4)$ (**8j**) in quantitative yield, while the reaction with MeI proceeds analogously to give the corresponding salt $[\text{Fe}_2\text{Cp}_2(\mu\text{-CyPNHNMeCH})(\mu\text{-CO})(\text{CO})]\text{I}$ (**8k**) in ca. 1 h at room temperature (Chart 7).

The NMR data available for compounds **8** (Table 2 and Experimental Section) reveal a close structural relation with their precursor **7g**. In particular, these complexes are also obtained as a mixture of the corresponding *cis* and *trans* isomers (Chart 7), although the *cis/trans* ratio is different from that in **7g** (ca. 10:1 in dichloromethane), and only in the case of the methyl derivative is this ratio dependent on the solvent. Apart from this, the pattern of the C–O stretching bands for the major isomer (the bands for the minor isomers are barely visible) in compounds **8** is analogous to that of the major (*cis*) isomer of **7g**, but shifted some 25–30 cm^{-1} upward, thus indicating the retention of one terminal and one bridging ligand. This is paralleled by the observation of carbonyl resonances at ca. 211 and 262 ppm, respectively, in the corresponding ^{13}C NMR spectra, which also display a now more deshielded iminoacyl resonance at ca. 215 ppm. Finally, the ^1H NMR spectra display the expectedly deshielded resonances for the corresponding CH and NH

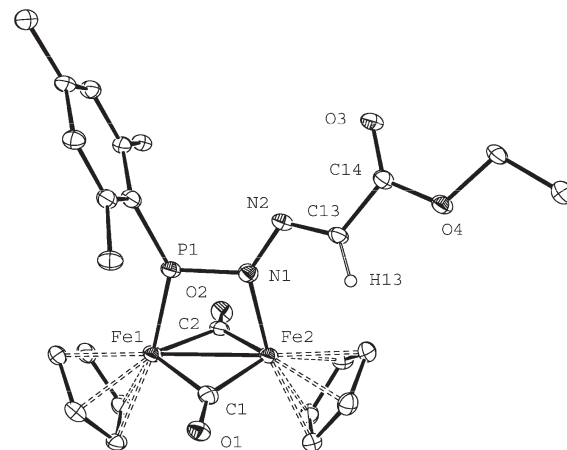


Figure 5. ORTEP diagram (30% probability) of compound **9**, with H atoms (except H13) omitted for clarity.

Table 5. Selected Bond Lengths (Å) and Angles (deg) for Compound **9**

Fe(1)–Fe(2)	2.514(1)	Fe(1)–C(1)–Fe(2)	81.9(2)
Fe(1)–P(1)	2.096(2)	Fe(1)–C(2)–Fe(2)	82.3(2)
Fe(1)–C(1)	1.976(5)	Fe(1)–Fe(2)–N(1)	79.5(1)
Fe(1)–C(2)	1.942(6)	Fe(2)–Fe(1)–P(1)	76.11(5)
Fe(2)–C(1)	1.856(6)	Fe(1)–P(1)–N(1)	102.4(2)
Fe(2)–C(2)	1.877(5)	P(1)–N(1)–Fe(2)	101.9(2)
Fe(2)–N(1)	2.028(5)	P(1)–N(1)–N(2)	121.3(4)
P(1)–N(1)	1.643(4)	P(1)–Fe(1)–C(1)	85.2(2)
N(1)–N(2)	1.372(6)	P(1)–Fe(1)–C(2)	84.5(2)
N(2)–C(13)	1.279(7)	N(1)–N(2)–C(13)	116.2(4)
C(13)–C(14)	1.492(7)	N(2)–C(13)–C(14)	118.7(5)
C(13)–H(13)	0.96(6)	N(2)–C(13)–H(13)	120(3)

protons, whereas, in the case of **8k**, the new methyl group gives rise to a resonance at 3.61 ppm.

Solid-State and Solution Structure of Compound 9. The molecular structure of this compound in the crystal (Figure 5 and Table 6) displays two iron cyclopentadienyl moieties bridged by two carbonyls and a phosphazadiene ligand, the latter being bound through phosphorus to one metal and through the contiguous nitrogen atom to the second metal. This establishes the main difference from the coordination mode proposed for **4** and crystallographically determined for $[\text{Mn}_2(\mu\text{-}^t\text{Pr}_2\text{NPN}_2\text{CPh}_2)(\text{CO})_8]$ ³¹ (mode **R** in Chart 3) and, therefore, constitutes a novel coordination mode of the phosphazadiene ligands. The bridging carbonyls in **9** define an almost planar Fe_2C_2 rhombus, and the PNNC chain of the bridging ligand defines a second plane perpendicular to the former plane and containing the metals. The overall coordination sphere of the metals in **9** is thus very similar to that displayed by the isoelectronic diphosphine-bridged complexes of the type $[\text{Fe}_2\text{Cp}_2(\mu\text{-CO})_2(\mu\text{-L}_2)]$, and accordingly, the intermetallic separation of 2.514(1) Å is comparable (ca. 2.51 Å for $\text{L}_2 = (\text{EtO})_2\text{POP}(\text{OEt})_2$,¹⁶ $\text{Ph}_2\text{P}(\text{CH}_2)_2\text{PPh}_2$).²⁴ The Fe–P distance of 2.096(1) Å is somewhat shorter than those measured for the above complexes or for related phosphine and phosphite complexes of the type $[\text{Fe}_2\text{Cp}_2(\mu\text{-CO})_2(\text{CO})(\text{L})]$,^{18b,25} with values of ca. 2.11–2.21 Å, and also shorter than those in the aminophosphide complexes **7e,f** (2.11–2.20 Å). Thus it would be tempting to interpret this

(24) Shade, J. E.; Pearson, W. H.; Brown, J. E.; Bitterwolf, T. E. *Organometallics* **2005**, *14*, 157.

(25) (a) Cotton, F. A.; Frenz, B. A.; White, A. J. *Inorg. Chem.* **1974**, *13*, 1407. (b) Alvarez, C. M.; Galán, B.; García, M. E.; Riera, V.; Ruiz, M. A.; Vaissermann, J. *Organometallics* **2003**, *22*, 5504.

(23) Malisch, W.; Grün, K.; Fried, A.; Reich, W.; Pfister, H.; Huttner, G.; Zsolnai, L. *J. Organomet. Chem.* **1998**, *566*, 271.

Table 6. Crystal Data for New Compounds

	2a.1	3	7e	9·0.5C ₆ H ₁₄
mol formula	C ₂₀ H ₂₃ Fe ₂ N ₂ O ₃ P	C ₂₀ H ₂₄ BF ₄ Fe ₂ N ₂ O ₃ P	C ₂₂ H ₂₇ Fe ₂ N ₂ O ₄ P	C ₃₇ H ₅₂ Fe ₂ N ₂ O ₄ P
mol wt	482.07	569.89	526.13	731.48
cryst syst	monoclinic	orthorhombic	triclinic	monoclinic
space group	<i>P</i> 2 ₁ / <i>n</i>	<i>P</i> 2 ₁ 2 ₁ 2 ₁	<i>P</i> $\bar{1}$	<i>C</i> 2/ <i>c</i>
radiation (\AA , \AA)	0.71073	0.71073	0.71073	1.54184
<i>a</i> , \AA	12.018(2)	10.723(2)	11.0876(3)	19.9691(18)
<i>b</i> , \AA	11.601(2)	12.889(2)	13.7702(4)	10.0163(8)
<i>c</i> , \AA	14.223(2)	16.683(3)	15.7119(5)	36.114(3)
α , deg	90	90	72.167(2)	90
β , deg	91.310(3)	90	72.183(2)	98.256(8)
γ , deg	90	90	77.026(2)	90
<i>V</i> , \AA^3	1982.5(6)	2305.7(7)	2151.32(11)	7148.6(11)
<i>Z</i>	4	4	4	8
calcd density, g cm ⁻³	1.615	1.642	1.624	1.359
absorp coeff, mm ⁻¹	1.568	1.385	1.456	7.252
temperature, K	120(2)	120(2)	100(2)	100(2)
θ range (deg)	2.19–26.45	2.0–27.2	1.41–26.02	4.47–74.21
index ranges (<i>h</i> , <i>k</i> , <i>l</i>)	–14, 15; 0, 14; 0, 17	–13, 13; 0, 16; 0, 21	–12, 13; –15, 16; 0, 19	–21, 23; –11, 11; –43, 44
no. of reflns collected	22 694	36 457	34 016	26 811
no. of indep reflns (<i>R</i> _{int})	4286 (0.0602)	5128 (0.0471)	8466 (0.0582)	6640 (0.0826)
reflns with <i>I</i> > 2 σ (<i>I</i>)	2990	4689	5364	4576
<i>R</i> indexes [data with <i>I</i> > 2 σ (<i>I</i>)] ^a	<i>R</i> ₁ = 0.0339 <i>wR</i> ₂ = 0.0681 ^b	<i>R</i> ₁ = 0.0238 <i>wR</i> ₂ = 0.0496 ^c	<i>R</i> ₁ = 0.0548 <i>wR</i> ₂ = 0.1372 ^d	<i>R</i> ₁ = 0.0655 <i>wR</i> ₂ = 0.1431 ^e
<i>R</i> indexes (all data) ^a	<i>R</i> ₁ = 0.0543 <i>wR</i> ₂ = 0.0733 ^b	<i>R</i> ₁ = 0.0281 <i>wR</i> ₂ = 0.051 ^c	<i>R</i> ₁ = 0.0956 <i>wR</i> ₂ = 0.1523 ^d	<i>R</i> ₁ = 0.0996 <i>wR</i> ₂ = 0.1587 ^e
GOF	1.033	1.083	1.078	1.04
no. of restraints/params	0/261	0/311	0/626	0/430
$\Delta\rho$ (max., min.), e \AA^{-3}	0.427, –0.342	0.255, –0.248	1.234, –1.21	0.818, –0.772

^a $R = \sum |F_o| - |F_c| / \sum |F_o|$. $wR = [\sum w(|F_o|^2 - |F_c|^2)^2 / \sum w|F_o|^2]^{1/2}$. $w = 1/[\sigma^2(F_o^2) + (aP)^2 + bP]$ where $P = (F_o^2 + 2F_c^2)/3$. ^b $a = 0.0280$, $b = 1.1802$. ^c $a = 0.0213$, $b = 0.5229$. ^d $a = 0.0815$, $b = 0.0000$. ^e $a = 0.0420$, $b = 64.8613$.

shortening effect as an indication of the presence of some multiplicity in the Fe–P bond. Actually, the fact that the ³¹P chemical shift in **9** is some 120 ppm higher than that in **4** reinforces this interpretation. Moreover, the presence of some multiplicity in the Fe–P bond would possibly be accompanied by a reduction in the multiplicity of the P–N bond. Indeed, the value of 1.64(3) \AA for the P–N(1) length in **9** is intermediate between the values measured for compound **2a.1** (1.612(1) \AA , formally a double bond) and compounds **7e,f** (ca. 1.70 \AA , formally a single bond). As for the N–Fe length of 2.028(5) \AA , it can be considered as normal for a single bond involving sp²-hybridized N atoms, being comparable to the corresponding length in the phosphinimine complex [Fe₂(μ -Cl)₂Cl₂(N-(P^{*i*}Pr₃)CH₂SPh)₂] (2.033(2) \AA) and related iron complexes.²⁶ Due to the different donor properties of the P and N ligand sites in **9**, the electron density at the metal centers has to be balanced by a slightly asymmetric coordination of the bridging carbonyls, closer to Fe(2), the iron atom bearing the poorer donor. The interatomic N–N and N–C separations (1.372(6) and 1.279(7) \AA , respectively) are comparable to those in the complexes **2a.1** and **7e,f** previously discussed and, therefore, can be considered consistent with the formulation of single and double bonds, respectively.

The spectroscopic data in solution for **9** are consistent with its solid-state structure. We have already mentioned the strong deshielding of the P nucleus compared to that in complex **4**, this being attributed to the different coordination modes that the phosphadiazadiene ligand adopts in these two molecules, and the striking difference in the colors of these compounds (purple for **4**, green for **9**) might have a similar origin. As expected, the IR spectrum exhibits two

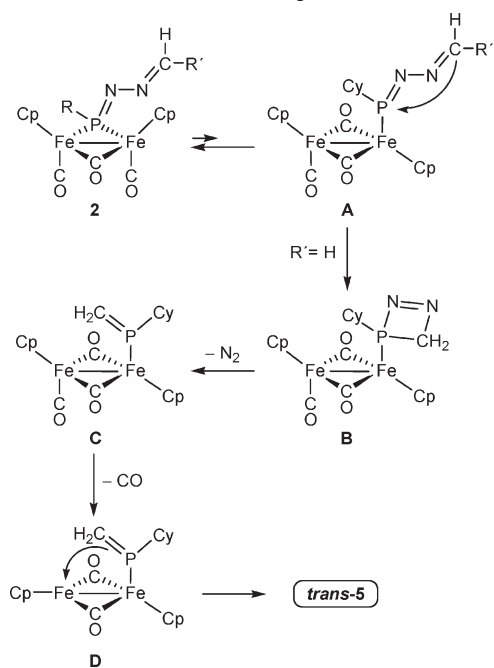
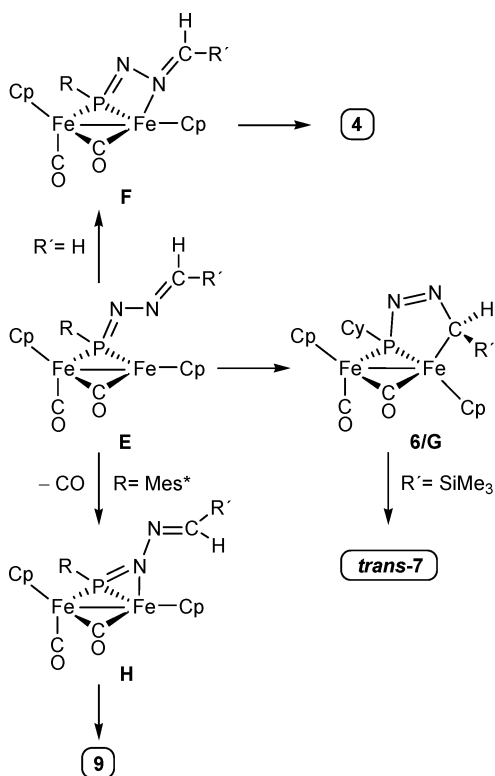
C–O stretching bands in the region of the bridging ligands, with the pattern characteristic of M₂(μ -CO)₂ oscillators with almost antiparallel CO ligands, as found for **4**. Finally, the NMR data indicate the retention of an effective symmetry plane containing the Fe and P atoms, while the uncoordinated methylenic group in **9** displays chemical shifts (δ_C 133.9 ppm, δ_H 6.22 ppm) comparable to those of complexes **2**.

Pathways in the Photochemical Reactions of the Phosphadiazadiene Complexes 2. In the preceding sections we have seen that the photochemical treatment of complexes **2** can induce many different rearrangements involving the phosphadiazadiene ligand. Although we have detected no intermediates in these reactions, we can propose reasonable elemental steps to account for the formation of all the isolated products, including their stereochemistry (Schemes 1 and 2).

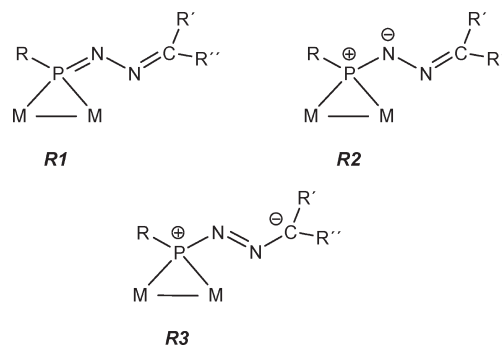
First of all, it should be recognized that the residual donor ability of the *P:P*-bound phosphadiazadiene ligand in compounds **2** is not restricted to their lone-pair-bearing N atoms, but also might involve its methylenic carbon. This can be grasped by taking into account the different canonical forms contributing to the electronic structure of the ligand (Chart 9). In particular the formal charges in **R3** illustrate the electron-rich nature of this carbon atom while emphasizing the electrophilic properties of the P atom.

In order to explain the formation of the phosphalkene complex **5**, we first propose that, at least under photochemical conditions, the complexes **2** would partially rearrange into the corresponding isomers having the P-donor ligand coordinated in a terminal fashion (**A** in Scheme 1). This is completely analogous to the thermal equilibrium recently observed between the terminal and bridged isomers of the oxophosphinidene complex [Fe₂Cp₂(CO)₃{P(O)Mes*}]⁸. The intermediate **A**, having now a low-coordination P center, might then undergo an intramolecular attack of the

(26) (a) LePichon, L.; Stephan, D. W. *Inorg. Chem.* **2001**, *40*, 3827. (b) Mai, H. J.; Wocadlo, S.; Kang, H. C.; Massa, W.; Dehnicke, K.; Maichle-Moösmser, C.; Strähle, J.; Fenske, D. *Z. Anorg. Allg. Chem.* **1995**, *621*, 705.

Scheme 1. Denitrogenation Pathway in the Photochemical Reactions of Compounds 2**Scheme 2. Reaction Pathways in the Photochemical Formation of Compounds 4–9**

electron-rich methylenic carbon to phosphorus, to yield a phosphine ligand having a very strained four-membered PNNC ring (**B** in Scheme 1). This would force its denitrogenation to give a *P*-bound phosphalkene complex **C**, which, under the action of UV light, would dissociate a CO molecule to give the phosphalkene-bridged complex **5**, initially in its *trans*-dicarbonyl form. However, as noted

Chart 9

before, compound **5** is obtained as a mixture of *cis* and *trans* isomers in a ratio *cis/trans* of ca. 10:1. This is likely to follow from a photochemically induced and reversible *trans/cis* isomerization in the final product, comparable to those previously observed in related species such as phosphide- and thiolate-bridged complexes of the type $[\text{Fe}_2\text{Cp}_2(\mu\text{-H})(\mu\text{-PR}_2)(\text{CO})_2]$ (*trans* to *cis*)^{27,28} and $[\text{Fe}_2\text{Cp}_2(\mu\text{-SR})_2(\text{CO})_2]$ (*cis* to *trans*).²⁹

The generation of significant amounts of the terminal isomer **A** upon photolysis of compounds **2** also gives a rationale for the observed photochemical decomposition of these complexes to yield variable amounts of $[\text{Fe}_2\text{Cp}_2(\text{CO})_4]$. Due to the absence of a bridging P atom in the intermediate **A**, it might be anticipated that this isomer might easily undergo, under photolytic conditions, the homolytic cleavage of the Fe–Fe bond to yield, *inter alia*, $\text{FeCp}(\text{CO})_2$ radicals that would rapidly recombine to give the iron dimer, thus paralleling the extensively studied photochemistry of the latter species.³⁰

In the presence of a substituent at the methylenic carbon in the intermediate **A**, the cyclization step preceding denitrogenation might be disfavored possibly by the steric hindrance induced by this substituent at intermediate **B**. As a result, the photochemically activated compound **2** would rather dissociate a CO molecule to give an unsaturated intermediate **E** (Scheme 2). This process would be also operative for the unsubstituted compound **2a.1** (in fact it seems to be the dominant pathway even in that case). The nature of the products finally isolated suggests that the intermediates **E** would eliminate its coordinative and electronic deficiency in three different ways, depending on the substituents at the bridging ligand. For cyclohexyl compounds, in the absence of substituents at the methylenic carbon, the phosphadiazadiene ligand might coordinate its C-bound nitrogen atom, to give a *P:P,N*-bridged intermediate **F** structurally related to complexes **7**, but having a strained four-membered PNNFe ring, which then would rearrange into its *P:N*-bridged isomer **4**, with an unstrained five-membered PN_2Fe_2 ring.

When a substituent is present at the methylenic carbon, the formation of the corresponding intermediate **F** would be disfavored because of the implied close approach of the substituent to a cyclopentadienyl ligand. Then, the unsaturation at the intermediate **E** would be eliminated by the

(27) (a) Brunner, H.; Peter, H. *J. Organomet. Chem.* **1990**, 393, 411. (b) Brunner, H.; Rötzer, M. *J. Organomet. Chem.* **1992**, 425, 119.

(28) Alvarez, C. M.; García, M. E.; Ruiz, M. A.; Connelly, N. G. *Organometallics* **2004**, 23, 4750.

(29) Bitterwolf, T. E.; Scallorn, W. B.; Li, B. H. *Organometallics* **2000**, 19, 3280.

(30) Bitterwolf, T. E. *Coord. Chem. Rev.* **2000**, 206–207, 419.

coordination of the nucleophilic methylenic carbon in a terminal way, thus giving the isolable complex **6** ($R = \text{CO}_2\text{Et}$) or a similar but unstable intermediate **G** ($R = \text{SiMe}_3$). Initially, these species should display a *transoid* arrangement of the terminal ligands, which seems to be the case of the major isomer for **6** according to the IR spectrum of this complex, as discussed above. Finally, the intermediate **G** would undergo a fast 1,3-shift of the SiMe_3 group to yield the aminophosphide-iminoacyl derivative **7f**, initially in its *transoid* form. As discussed for **5**, under photochemical activation, a reversible *trans* to *cis* isomerization would finally account for the observed mixture of isomers. Incidentally, this is in agreement with the fact that the major isomer in the related complex **7e**, which is not formed photochemically, but through a *thermal* reaction of **6** on the surface of alumina, exhibits the same arrangement of terminal ligands (*trans*) as its precursor **6**. Although the 1,3-shift responsible for the formation of **7f** is not a common rearrangement, there are some precedents of related SiMe_3 shifts involving two N atoms or C and N atoms, and even 1,4-shifts between O and N atoms.³¹ Besides this, we should note the parallelism between the formation of the phosphide-iminoacyl complex **7f** (reaction of the phosphinidene **1a** with a diazoalkane followed by photochemically induced decarbonylation and 1,3- SiMe_3 shift) and the thermal formation of the mononuclear phosphine-iminoacyl complex $[\text{MoCp}(\text{CO})_2\{\text{Bu}_2\text{PNHNC}(\text{CO}_2\text{Et})\}]$ from a terminal phosphide complex with ethyldiazoacetate followed by decarbonylation and 1,3-H shift at the presumed (undetected) diazoalkane adduct initially formed.²³ In the formation of compounds **7**, however, no 1,3-H shift seems to be feasible at the intermediate stages **6/G** without apparent reason, although it is clear that the observed SiMe_3 shift yields an isomer having the bulky silyl group pointing away from the dimetal center, therefore much more favored on steric grounds.

The third possible way to remove the unsaturation in the intermediate **E** is the coordination of the P-bound nitrogen atom. This might be viewed as the least likely alternative, but it is the one keeping a substituted methylenic group as far away as possible from the rest of the molecule, and therefore perhaps the least disfavored option in the presence of a really bulky substituent at phosphorus such as the supermesityl group. Thus, in the case of compound **2c.2** the corresponding intermediate **E** would first give a *P:P,N*-bridged intermediate **H** with a structure related to that of the phosphalkene complex **5**, then rearranging into the *P:N*-bridged isomer **9**, now having a less strained four-membered FePNFe ring. The fact that compound **9** displays a structure different from those of **4**, **6**, or **7** might be thus explained on kinetic grounds. In addition, an analysis of the crystal structure of **9** reveals the presence of close contacts between the *ortho* ^tBu groups of the substituent at phosphorus and the cyclopentadienyl ligand bound to the same metal atom. Therefore it can be guessed that any hypothetical structure for this compound analogous to that of **4** would be thermodynamically disfavored too, because of the strong Mes^*/Cp repulsions derived from the closer approach between these groups.

(31) (a) Cole, M. L.; Junk, P. C. *Dalton Trans.* **2003**, 2109. (b) Hitchcock, P. B.; Lappert, M. F.; Wei, X. H. *J. Organomet. Chem.* **2003**, 683, 83. (c) Tobita, H.; Matsuda, A.; Hashimoto, H.; Ueno, K.; Ogino, H. *Angew. Chem., Int. Ed.* **2004**, 43, 221. (d) Yu, X.; Xue, Z. L. *Inorg. Chem.* **2005**, 44, 1505. (e) Wang, Z. X.; Chai, Z. Y.; Li, Y. X. *J. Organomet. Chem.* **2005**, 690, 4252. (f) Ito, S.; Miyake, H.; Yoshifuji, M. *Eur. J. Inorg. Chem.* **2007**, 22, 3491.

Concluding Remarks

The phosphinidene complexes $[\text{Fe}_2\text{Cp}_2(\mu\text{-PR})(\mu\text{-CO})(\text{CO})_2]$ react readily with different diazoalkane molecules $\text{N}_2\text{CR}'\text{R}''$ to yield the corresponding derivatives $[\text{Fe}_2\text{Cp}_2(\mu\text{-RPN}_2\text{CR}'\text{R}'')(\mu\text{-CO})(\text{CO})_2]$, which display a novel *P:P*-bridging coordination mode of the phosphadiazadiene ligand resulting from a biphilic P–N interaction of the phosphinidene with the terminal nitrogen of the diazoalkane. Under photochemical activation, the new complexes undergo decarbonylation and different rearrangements of the phosphadiazadiene ligands that are strongly influenced by the steric effects of the substituents present at phosphorus and at the methylenic carbon of the former diazoalkane molecule. The diazomethane derivative, having the smallest steric demands, can evolve in two different ways, one of them implying the nucleophilic attack of the methylenic carbon to the phosphorus atom and eventually releasing dinitrogen to yield a phosphalkene derivative. The formation of all other products can be explained by assuming the photochemical generation of a common unsaturated dicarbonyl intermediate that, as the steric demands of the substituents there present increase, reaches its electronic saturation through the coordination to the metal center of the following atoms (in order of preference): C-bound nitrogen < methylenic carbon < P-bound nitrogen. The two last options lead to novel bridging coordination modes of the phosphadiazadiene ligand. Moreover, the coordination of the methylenic carbon to the metal center facilitates 1,3-shifts between the C and N atoms of the ligand to yield novel aminophosphide-iminoacyl derivatives.

Experimental Section

General Procedures and Starting Materials. All manipulations and reactions were carried out under a nitrogen (99.995%) atmosphere using standard Schlenk techniques. Solvents were purified according to literature procedures and distilled prior to use.³² Petroleum ether refers to that fraction distilling in the range 338–343 K. Dichloromethane solutions of the compounds $[\text{Fe}_2\text{Cp}_2(\mu\text{-PR})(\mu\text{-CO})(\text{CO})_2]$ ($\text{Cp} = \eta^5\text{-C}_5\text{H}_5$; $R = \text{Cy}$ (**1a**), Ph (**1b**), 2,4,6- $\text{C}_6\text{H}_2\text{Bu}_3$ (**1c**)) were prepared *in situ* as described previously.^{6,8} Diethyl ether solutions of diazomethane were prepared *in situ* also by literature methods,³³ and diphenyldiazomethane was prepared as reported previously.³⁴ All other reagents were obtained from the usual commercial suppliers and used as received. Photochemical experiments were performed using jacketed quartz or Pyrex Schlenk tubes, cooled by tap water (ca. 288 K). A 400 W mercury lamp placed ca. 1 cm away from the Schlenk tube was used for all the experiments. Chromatographic separations were carried out using jacketed columns cooled by tap water (ca. 288 K) or by a closed 2-propanol circuit, kept at the desired temperature with a cryostat. Commercial aluminum oxide (activity I, 150 mesh) was degassed under vacuum prior to use. The latter was mixed under nitrogen with the appropriate amount of water to reach the activity desired. IR C–O stretching frequencies were measured in solution and are referred to as $\nu(\text{CO})$. Nuclear magnetic resonance (NMR) spectra were routinely recorded at 300.13 (¹H), 121.50 (³¹P{¹H}), or 75.48 MHz (¹³C{¹H}) at 290 K in CD_2Cl_2 solutions unless otherwise is stated. Chemical shifts (δ) are given in ppm, relative to internal tetramethylsilane (¹H, ¹³C)

(32) Armarego, W. L. F.; Chai, C. *Purification of Laboratory Chemicals*, 5th ed.; Butterworth-Heinemann: Oxford, U.K., 2003.

(33) Vogel, A. I. *Textbook for Practical Organic Chemistry*, 4th ed.; Longman: London, U.K., 1978.

(34) Millar, J. B. *J. Org. Chem.* **1959**, 24, 560.

or external 85% aqueous H_3PO_4 (^{31}P). Coupling constants (J) are given in Hz. The magnetic susceptibility of compound **6** was measured in CD_2Cl_2 solution by the NMR method developed by Evans.²⁰ The molar magnetic susceptibility thus obtained (χ^{M}) was then corrected for the diamagnetic contribution as estimated from atomic susceptibilities.³⁵ The resulting value (χ^{C}) was then used for calculating the effective magnetic moment (μ_{eff}) as usual.

Preparation of $[\text{Fe}_2\text{Cp}_2(\mu\text{-CyPN}_2\text{CH}_2)(\mu\text{-CO})(\text{CO})_2]$ (2a.1**).** A large excess of a freshly prepared Et_2O solution of N_2CH_2 was added to a freshly prepared solution of complex **1a** (ca. 0.050 g, 0.114 mmol) in dichloromethane (5 mL) at 273 K, and the mixture was stirred at that temperature for 15 min to give a dark green solution. The solvent was then removed under vacuum, and the residue was washed with petroleum ether (2×3 mL) to give compound **2a.1** as a green microcrystalline solid (0.051 g, 91%). The crystals used in the diffractometric study were grown by the slow diffusion of a layer of petroleum ether into a toluene solution of the complex at 253 K. Anal. Calcd for $\text{C}_{20}\text{H}_{23}\text{Fe}_2\text{N}_2\text{O}_3\text{P}$: C, 49.83; H, 4.81; N, 5.81. Found: C, 49.62; H, 4.68; N, 5.67. ^1H NMR: δ 7.10 (dd, $J_{\text{HH}} = 15$, $J_{\text{HP}} = 2$, 1H, CH_2), 6.43 (d, $J_{\text{HH}} = 15$, 1H, CH_2), 5.11 (s, 10H, Cp), 2.42–1.18 (m, 11H, Cy). $^{13}\text{C}\{^1\text{H}\}$ NMR: δ 270.1 (s, $\mu\text{-CO}$), 212.1 (d, $J_{\text{CP}} = 11$, FeCO), 133.7 (d, $J_{\text{CP}} = 51$, CH_2), 87.4 (s, Cp), 55.5 [d, $J_{\text{CP}} = 53$, $\text{C}^1(\text{Cy})$], 32.1 [d, $J_{\text{CP}} = 6$, $\text{C}^2(\text{Cy})$], 27.8 [d, $J_{\text{CP}} = 11$, $\text{C}^3(\text{Cy})$], 26.5 [s, $\text{C}^4(\text{Cy})$].

Preparation of $[\text{Fe}_2\text{Cp}_2(\mu\text{-CyPN}_2\text{CH}(\text{CO}_2\text{Et}))(\mu\text{-CO})(\text{CO})_2]$ (2a.2**).** Neat $\text{N}_2\text{CH}(\text{CO}_2\text{Et})$ (10 μL , 0.095 mmol) was added to a freshly prepared solution of complex **1** (ca. 0.040 g, 0.091 mmol) in dichloromethane (5 mL), and the mixture was stirred at room temperature for 5 min to give a dark green solution. Workup as described for **2a.1** gave compound **2a.2** as a green microcrystalline solid (0.048 g, 95%). Anal. Calcd for $\text{C}_{25}\text{H}_{27}\text{Fe}_2\text{N}_2\text{O}_5\text{P}$: C, 49.85; H, 4.91; N, 5.06. Found: C, 49.69; H, 4.87; N, 5.98. ^1H NMR (CDCl_3): δ 7.75 (s, 1H, CH), 5.13 (s, 10H, Cp), 4.21 (c, $J_{\text{HH}} = 7$, 2H, OCH_2), 2.47 (m, 1H, Cy), 2.25 (m, 2H, Cy), 1.90 (m, 2H, Cy), 1.70–1.20 (m, 6H, Cy), 1.27 (t, $J_{\text{HH}} = 7$, 3H, Me). $^{13}\text{C}\{^1\text{H}\}$ NMR (100.62 MHz, CDCl_3): δ 267.5 (s, $\mu\text{-CO}$), 210.8 (d, $J_{\text{CP}} = 13$, FeCO), 166.0 (s, CO_2Et), 130.0 (d, $J_{\text{CP}} = 55$, CH), 87.6 (s, Cp), 59.6 (s, OCH_2), 53.6 [d, $J_{\text{CP}} = 47$, $\text{C}^1(\text{Cy})$], 31.6 [d, $J_{\text{CP}} = 7$, $\text{C}^2(\text{Cy})$], 27.2 [d, $J_{\text{CP}} = 11$, $\text{C}^3(\text{Cy})$], 25.7 [s, $\text{C}^4(\text{Cy})$], 14.5 (s, Me).

Preparation of $[\text{Fe}_2\text{Cp}_2(\mu\text{-CyPN}_2\text{CH}(\text{SiMe}_3))(\mu\text{-CO})(\text{CO})_2]$ (2a.3**).** A solution of $\text{N}_2\text{CH}(\text{SiMe}_3)$ (70 μL of a 2 M solution in petroleum ether, 0.140 mmol) was added to a freshly prepared solution of complex **1** (ca. 0.040 g, 0.091 mmol) in dichloromethane (5 mL), and the mixture was stirred at room temperature for 16 h to give a dark green solution. Workup as described for **2a.1** gave compound **2a.3** as a green microcrystalline solid (0.045 g, 90%). Anal. Calcd for $\text{C}_{23}\text{H}_{31}\text{Fe}_2\text{N}_2\text{O}_3\text{PSi}$: C, 49.84; H, 5.64; N, 5.05. Found: C, 49.60; H, 5.59; N, 4.90. ^1H NMR: δ 7.75 (s, 1H, CH), 5.13 (s, 10H, Cp), 2.50–1.10 (m, 11H, Cy), 0.15 (s, 9H, Me).

Preparation of $[\text{Fe}_2\text{Cp}_2(\mu\text{-CyPN}_2\text{CPh}_2)(\mu\text{-CO})(\text{CO})_2]$ (2a.4**).** A solution of N_2CPh_2 (0.025 g, 0.13 mmol) in dichloromethane (2 mL) was added to a freshly prepared solution of complex **1** (ca. 0.040 g, 0.091 mmol) in dichloromethane (5 mL), and the mixture was stirred at room temperature for 5 min to give a dark green solution. Workup as described for **2a.1** gave compound **2a.4** as a green microcrystalline solid (0.052 g, 90%). Anal. Calcd for $\text{C}_{32}\text{H}_{31}\text{Fe}_2\text{N}_2\text{O}_3\text{P}$: C, 60.60; H, 4.93; N, 4.42. Found: C, 60.51; H, 4.87; N, 4.28. ^1H NMR: δ 7.56–7.18 (m, 10H, Ph), 5.13 (s, 10H, Cp), 2.25–1.58 (m, 11H, Cy).

Preparation of $[\text{Fe}_2\text{Cp}_2(\mu\text{-PhPN}_2\text{CH}(\text{CO}_2\text{Et}))(\mu\text{-CO})(\text{CO})_2]$ (2b.2**).** The procedure is identical to that described for compound **2a.2**, but using complex **1b** (ca. 0.040 g, 0.092 mmol). This gave compound **2b.2** as a green microcrystalline solid (0.045 g,

89%). Anal. Calcd for $\text{C}_{23}\text{H}_{21}\text{Fe}_2\text{N}_2\text{O}_5\text{P}$: C, 50.40; H, 3.86; N, 5.11. Found: C, 50.17; H, 3.66; N, 5.02. ^1H NMR (CDCl_3): δ 7.90 (m, 2H, Ph), 7.51 (s, 1H, CH), 7.48–7.37 (m, 3H, Ph), 5.27 (s, 10H, Cp), 4.22 (q, $J_{\text{HH}} = 7$, 2H, OCH_2), 1.29 (t, $J_{\text{HH}} = 7$, 3H, Me).

Preparation of $[\text{Fe}_2\text{Cp}_2(\mu\text{-PhPN}_2\text{CH}(\text{SiMe}_3))(\mu\text{-CO})(\text{CO})_2]$ (2b.3**).** The procedure is identical to that described for compound **2a.3**, but using complex **1b** (ca. 0.030 g, 0.069 mmol) and a reaction time of 2 h. This gave compound **2b.3** as an air-sensitive green solid (0.045 g, 89%). ^1H NMR: δ 7.88 (m, 2H, Ph), 7.74 (s, CH), 7.44–7.20 (m, 3H, Ph), 5.25 (s, 10H, Cp), 0.14 (s, 9H, SiMe_3).

Preparation of $[\text{Fe}_2\text{Cp}_2(\mu\text{-PhPN}_2\text{CPh}_2)(\mu\text{-CO})(\text{CO})_2]$ (2b.4**).** The procedure is identical to that described for compound **2a.4**, but using complex **1b** (ca. 0.030 g, 0.069 mmol). This gave compound **2b.4** as a green microcrystalline solid (0.039 g, 92%). Anal. Calcd for $\text{C}_{32}\text{H}_{25}\text{Fe}_2\text{N}_2\text{O}_3\text{P}$: C, 61.18; H, 4.01; N, 4.46. Found: C, 60.97; H, 3.79; N, 4.23. ^1H NMR (400.13 MHz): δ 7.87 (m, 2H, Ph), 7.52–7.16 (m, 13H, Ph), 5.25 (s, 10H, Cp).

Preparation of $[\text{Fe}_2\text{Cp}_2(\mu\text{-Mes}^*\text{PN}_2\text{CH}(\text{CO}_2\text{Et}))(\mu\text{-CO})(\text{CO})_2]$ (2c.2**).** The procedure is identical to that described for compound **2a.2**, but using complex **1c** (ca. 0.040 g, 0.066 mmol). This gave compound **2c.2** as a green microcrystalline solid (0.043 g, 90%). Anal. Calcd for $\text{C}_{35}\text{H}_{45}\text{Fe}_2\text{N}_2\text{O}_5\text{P}$: C, 58.68; H, 3.91; N, 6.33. Found: C, 58.56; H, 4.05; N, 6.09. ^1H NMR (400.13 MHz): δ 7.36 (s, 1H, CH), 7.17 (d, $J_{\text{HP}} = 2$, 2H, C_6H_2), 5.25 (s, 10H, Cp), 4.24 (q, $J_{\text{HH}} = 7$, 2H, OCH_2), 1.67 (s, 18H, $o\text{-}^i\text{Bu}$), 1.32 (t, $J_{\text{HH}} = 7$, 3H, Me), 1.11 (s, 9H, $p\text{-}^i\text{Bu}$). $^{13}\text{C}\{^1\text{H}\}$ NMR (100.62 MHz): δ 269.1 (s, $\mu\text{-CO}$), 210.4 (d, $J_{\text{CP}} = 9$, FeCO), 166.6 (s, CO_2Et), 155.0 [d, $J_{\text{CP}} = 7$, $\text{C}^2(\text{C}_6\text{H}_2)$], 149.8 [s, $\text{C}^4(\text{C}_6\text{H}_2)$], 137.2 [d, $J_{\text{CP}} = 71$, $\text{C}^1(\text{C}_6\text{H}_2)$], 126.3 (d, $J_{\text{CP}} = 61$, CH), 123.5 [d, $J_{\text{CP}} = 12$, $\text{C}^3(\text{C}_6\text{H}_2)$], 90.2 (s, Cp), 59.9 (s, OCH_2), 41.8 [s, $\text{C}^1(o\text{-}^i\text{Bu})$], 34.3 [s, $\text{C}^2(o\text{-}^i\text{Bu})$], 31.2 [s, $\text{C}^1(p\text{-}^i\text{Bu})$], 30.8 [s, $\text{C}^2(p\text{-}^i\text{Bu})$], 14.8 (s, Me).

Preparation of $[\text{Fe}_2\text{Cp}_2(\mu\text{-CyPNHNC}_2\text{H}_5)(\mu\text{-CO})(\text{CO})_2](\text{BF}_4)$ (3**).** A slight excess of $\text{HBF}_4 \cdot \text{OEt}_2$ (12 μL of a 54% solution in Et_2O , 0.087 mmol) was added to a dichloromethane solution (5 mL) of compound **2a.1** (0.040 g, 0.083 mmol), and the mixture was stirred at room temperature for 5 min to give a red solution. The solvent was then removed under vacuum, and the residue was washed with Et_2O (3×4 mL) and then petroleum ether (2×4 mL) to give compound **3** as a red microcrystalline solid (0.044 g, 93%). The crystals used in the diffractometric study were grown by the slow diffusion of layers of toluene and petroleum ether into a dichloromethane solution of the complex at 253 K. Anal. Calcd for $\text{C}_{20}\text{H}_{24}\text{BF}_4\text{Fe}_2\text{N}_2\text{O}_3\text{P}$: C, 42.15; H, 4.24; N, 4.92. Found: C, 41.98; H, 4.05; N, 4.77. ^1H NMR: δ 8.80 (d, $J_{\text{HP}} = 17$, 1H, NH), 7.43 (d, $J_{\text{HH}} = 11$, 1H, CH_2), 6.68 (d, $J_{\text{HH}} = 11$, 1H, CH_2), 5.24 (s, 10H, Cp), 2.53–0.90 (m, 11H, Cy).

Photochemical Decarbonylation of Compound **2a.1.** A toluene solution (7 mL) of compound **2a.1** (0.200 g, 0.415 mmol) was irradiated with visible–UV light in a quartz Schlenk tube while keeping a gentle N_2 (99.9995%) purge at 288 K for 4 h to give a purple solution. The solvent was then removed under vacuum, and the residue was dissolved in a minimum of dichloromethane–petroleum ether (1:1) and chromatographed through an alumina column (activity IV) at 288 K. Elution with the same solvent mixture yielded a green fraction. Removal of solvents under vacuum from this fraction gave a 10:1 mixture of the *cis* and *trans* isomers of complex $[\text{Fe}_2\text{Cp}_2(\mu\text{-}\eta^2\text{-CyPCH}_2)(\mu\text{-CO})(\text{CO})]$ (**5**) as a green microcrystalline solid (0.039 g, 22%). Anal. Calcd for $\text{C}_{19}\text{H}_{23}\text{Fe}_2\text{O}_3\text{P}$: C, 53.56; H, 5.44. Found: C, 53.23; H, 5.15. Elution with dichloromethane–petroleum ether (5:1) yielded a purple fraction. Removal of solvents under vacuum from this fraction gave complex $[\text{Fe}_2\text{Cp}_2(\mu\text{-CyPN}_2\text{CH}_2)(\mu\text{-CO})_2]$ (**4**) as a purple microcrystalline solid (0.115 g, 61%) of low solubility in common solvents. Anal. Calcd for $\text{C}_{19}\text{H}_{23}\text{Fe}_2\text{N}_2\text{O}_3\text{P}$: C, 50.26; H, 5.11; N, 6.17. Found: C, 49.98; H, 5.02; N, 5.89. Spectroscopic data for compound **4**: ^1H NMR (400.13 MHz, CDCl_3): δ 4.70, 4.69 (2s, $2 \times 5\text{H}$, Cp), 4.21, 3.98 (2d, $J_{\text{HH}} = 7$, $2 \times 1\text{H}$, CH_2), 3.10 (m, 1H, Cy), 2.10–1.31 (m, 10H, Cy). Spectroscopic data for

(35) Oliver, K. *Molecular Magnetism*; Wiley: New York, 1992; Chapter 1.

cis-5: ^1H NMR (400.13 MHz): δ 4.59 (d, $J_{\text{HP}} = 1$, 5H, Cp), 4.50 (s, 5H, Cp), 2.70 [qt, $J_{\text{HH}} = J_{\text{HP}} = 12$, $J_{\text{HH}} = 3$, 1H, $\text{HC}^1(\text{Cy})$], 2.50, 2.23 (2 m, $2 \times 1\text{H}$, Cy), 2.08–1.37 (m, 8H, Cy), 1.52 (dd, $J_{\text{HH}} = 7$, $J_{\text{HP}} = 9$, 1H, PCH_2), –0.40 (dd, $J_{\text{HH}} = 7$, $J_{\text{HP}} = 6$, 1H, PCH_2). $^{13}\text{C}\{^1\text{H}\}$ NMR (100.62 MHz): 237.8 (d, $J_{\text{CP}} = 3$, $\mu\text{-CO}$), 219.3 (d, $J_{\text{CP}} = 33$, FeCO), 81.3, 78.4 (2s, Cp), 43.2 [d, $J_{\text{CP}} = 1$, $\text{C}^1(\text{Cy})$], 34.1 [s, $\text{C}^{2,6}(\text{Cy})$], 33.2 [d, $J_{\text{CP}} = 3$, $\text{C}^{6,2}(\text{Cy})$], 27.6 [d, $J_{\text{CP}} = 6$, $\text{C}^{3,5}(\text{Cy})$], 27.5 [d, $J_{\text{CP}} = 8$, $\text{C}^{5,3}(\text{Cy})$], 26.5 [s, $\text{C}^4(\text{Cy})$], 20.3 (d, $J_{\text{CP}} = 4$, PCH_2). Spectroscopic data for **trans-5:** ^1H NMR (400.13 MHz): δ 4.79, 4.48 (2s, $2 \times 5\text{H}$, Cp). $^{13}\text{C}\{^1\text{H}\}$ NMR (100.62 MHz): 81.1, 79.5 (2s, Cp); other resonances of this minor isomer could not be identified in the corresponding spectra due to its low proportion and/or superposition with the resonances of the major isomer.

Preparation of $[\text{Fe}_2\text{Cp}_2\{\mu\text{-CyPN}_2\text{CH}(\text{CO}_2\text{Et})\}(\mu\text{-CO})(\text{CO})]$ (6). A toluene solution (5 mL) of complex **2a.2** (0.060 g, 0.108 mmol) was irradiated with visible–UV light at 288 K in a quartz Schlenk tube for 1.5 h, while keeping a gentle N_2 purge, to give a dark green solution, which was filtered using a canula. The solvent was then removed from the filtrate under vacuum, and the residue was washed with petroleum ether (3 \times 4 mL) to give the paramagnetic complex **6** as a green microcrystalline solid (0.054 g, 97%). Anal. Calcd for $\text{C}_{22}\text{H}_{27}\text{Fe}_2\text{N}_2\text{O}_4\text{P}$: C, 50.22; H, 5.17; N, 5.32. Found: C, 50.07; H, 5.04; N, 5.13. $\mu_{\text{eff}}(\text{CD}_2\text{Cl}_2) = 2.75 \mu_{\text{B}}$.

Preparation of $\text{cis- and trans-}[\text{Fe}_2\text{Cp}_2\{\mu\text{-CyPNHNC}(\text{CO}_2\text{Et})\}(\mu\text{-CO})(\text{CO})]$ (7e). Compound **6** (0.054 g, 0.105 mmol) was dissolved in a minimum of dichloromethane–petroleum ether (1:2) and chromatographed through an alumina column (activity IV) at 263 K. Elution with dichloromethane yielded a green-brown fraction. Removal of solvents under vacuum from this fraction gave complex **trans-7e** as a green-brown solid (0.049 g, 86%). The crystals used in the diffractometric study were grown by the slow diffusion of layers of toluene and petroleum ether into a dichloromethane solution of the complex at 253 K. Elution with tetrahydrofuran–petroleum ether (1:1) yielded a pale green fraction, which gave analogously complex **cis-7e** as a green solid (0.005 g, 8%). Data for **trans-7e**: Anal. Calcd for $\text{C}_{22}\text{H}_{27}\text{Fe}_2\text{N}_2\text{O}_4\text{P}$: C, 50.22; H, 5.17; N, 5.32. Found: C, 50.10; H, 5.07; N, 5.26. ^1H NMR: δ 7.40 (d, br, $J_{\text{HP}} = 5$, 1H, NH), 4.58, 4.41 (2s, $2 \times 5\text{H}$, Cp), 4.15, 4.09 (2dq, $J_{\text{HH}} = 13$, $7, 2 \times 1\text{H}$, OCH_2), 3.06 (m, 1H, Cy), 2.60–1.97 (m, 5H, Cy), 1.90 (m, 1H, Cy), 1.65–1.43 (m, 4H, Cy), 1.31 (t, $J_{\text{HH}} = 7$, 3H, Me). $^{13}\text{C}\{^1\text{H}\}$ NMR (100.62 MHz): δ 266.0 (s, $\mu\text{-CO}$), 211.1 (d, $J_{\text{CP}} = 13$, FeCO), 191.9 (d, $J_{\text{CP}} = 11$, CCO_2Et), 170.3 (s, CO_2Et), 88.3, 86.2 (2s, Cp), 60.3 (s, OCH_2), 47.2 [d, $J_{\text{CP}} = 23$, $\text{C}^1(\text{Cy})$], 33.0 [s, $\text{C}^{2,6}(\text{Cy})$], 32.0 [s, $\text{C}^{6,2}(\text{Cy})$], 28.0, 27.7 [2d, $J_{\text{CP}} = 13$, C^3 and $\text{C}^5(\text{Cy})$], 26.4 [s, $\text{C}^4(\text{Cy})$], 14.8 (s, Me). Data for **cis-7e**: Anal. Calcd for $\text{C}_{22}\text{H}_{27}\text{Fe}_2\text{N}_2\text{O}_4\text{P}$: C, 50.22; H, 5.17; N, 5.32. Found: C, 50.17; H, 5.14; N, 5.21. ^1H NMR: δ 6.78 (d, br, $J_{\text{HP}} = 7$, 1H, NH), 4.70, 4.66 (2s, $2 \times 5\text{H}$, Cp), 4.15, 3.99 (2m, $2 \times 1\text{H}$, OCH_2), 2.96, 2.92, 2.56 (3m, $3 \times 1\text{H}$, Cy), 2.27–1.50 (m, 8H, Cy), 1.26 (t, $J_{\text{HH}} = 7$, 3H, Me).

Preparation of $[\text{Fe}_2\text{Cp}_2\{\mu\text{-CyPN}(\text{SiMe}_3)\text{NCH}\}(\mu\text{-CO})(\text{CO})]$ (7f). A toluene solution (6 mL) of complex **2a.3** (0.065 g, 0.117 mmol) was irradiated with visible–UV light at 288 K in a quartz Schlenk tube for 1 h, while keeping a gentle N_2 purge, to give a dark green solution, which was filtered using a canula. The solvent was then removed from the filtrate under vacuum, and the residue was washed with petroleum ether (2 \times 3 mL) to give a 3:1 mixture (by NMR) of the *cis* and *trans* isomers of complex **7f** as a green microcrystalline solid (0.060 g, 97%). Anal. Calcd for $\text{C}_{22}\text{H}_{31}\text{Fe}_2\text{N}_2\text{O}_2\text{PSi}$: C, 50.21; H, 5.94; N, 5.32. Found: C, 49.98; H, 5.76; N, 5.12. Spectroscopic data for **cis-7f**: ^1H NMR (400.13 MHz): δ 7.66 (d, $J_{\text{HP}} = 6$, 1H, CH), 4.73, 4.56 (2s, $2 \times 5\text{H}$, Cp), 3.55 [m, 1H, $\text{HC}^1(\text{Cy})$], 2.70–1.25 (m, 10H, Cy), 0.25 (s, 9H, Me). $^{13}\text{C}\{^1\text{H}\}$ NMR (100.63 MHz): δ 266.5 (d, $J_{\text{CP}} = 5$, $\mu\text{-CO}$), 214.1 (d, $J_{\text{CP}} = 21$, FeCO), 182.5 (d, $J_{\text{CP}} = 11$, CH), 85.5, 83.6 (2s, Cp), 50.2 [d, $J_{\text{CP}} = 10$, $\text{C}^1(\text{Cy})$], 33.6 [d, $J_{\text{CP}} = 3$, $\text{C}^{2,6}(\text{Cy})$], 30.6 [d, $J_{\text{CP}} = 2$, $\text{C}^{6,2}(\text{Cy})$], 27.9 [d, $J_{\text{CP}} = 11$, $\text{C}^{3,5}(\text{Cy})$], 27.7

[d, $J_{\text{CP}} = 14$, $\text{C}^{5,3}(\text{Cy})$], 26.6 [s, $\text{C}^4(\text{Cy})$], 1.2 (s, Me). Spectroscopic data for **trans-7f**: ^1H NMR (400.13 MHz): δ 8.20 (d, $J_{\text{HP}} = 6$, 1H, CH), 4.60, 4.34 (2s, $2 \times 5\text{H}$, Cp), 3.57 [m, 1H, $\text{HC}^1(\text{Cy})$], 2.70–1.25 (m, 10H, Cy), 0.38 (s, 9H, Me). $^{13}\text{C}\{^1\text{H}\}$ NMR (100.63 MHz): δ 269.8 (d, $J_{\text{CP}} = 6$, $\mu\text{-CO}$), 211.7 (d, $J_{\text{CP}} = 21$, FeCO), 191.8 (d, $J_{\text{CP}} = 11$, CH), 88.1, 85.5 (2s, Cp), 46.0 [d, $J_{\text{CP}} = 16$, $\text{C}^1(\text{Cy})$], 33.2 [d, $J_{\text{CP}} = 2$, $\text{C}^{2,6}(\text{Cy})$], 30.9 [d, $J_{\text{CP}} = 4$, $\text{C}^{6,2}(\text{Cy})$], 26.4 [s, $\text{C}^4(\text{Cy})$], 2.1 (s, Me); other resonances for this isomer were obscured by those of the major isomer.

Preparation of $[\text{Fe}_2\text{Cp}_2(\mu\text{-CyPNHNCH})(\mu\text{-CO})(\text{CO})]$ (7g). Degassed water (4 mL, 0.222 mmol) was added to a toluene solution (5 mL) of compound **7f** (0.065 g, 0.124 mmol), and the mixture was stirred for 30 min to give a green solution. The solvent was then removed under vacuum, and the residue was dissolved in a minimum of dichloromethane–petroleum ether (1:1) and chromatographed through an alumina column (activity IV) at 288 K. Elution with dichloromethane yielded a green fraction. Removal of solvents under vacuum from this fraction gave a mixture of the *cis* and *trans* isomers of complex **7g** as a green microcrystalline solid (0.051 g, 91%). These isomers interconvert in dichloromethane solution, with the equilibrium ratio being ca. 4:1 at 253 K. Anal. Calcd for $\text{C}_{19}\text{H}_{23}\text{Fe}_2\text{N}_2\text{O}_2\text{P}$: C, 50.26; H, 5.11; N, 6.17. Found: C, 50.18; H, 4.89; N, 6.12. Spectroscopic data for **cis-7g**: ^1H NMR (400.13 MHz): δ 7.82 (s, br, 1H, CH), 6.42 (s, br, 1H, NH), 4.67, 4.61 (2s, $2 \times 5\text{H}$, Cp), 2.95 (m, 1H, Cy), 2.73, 2.56 (2 m, $2 \times 1\text{H}$, Cy), 2.24–1.42 (m, 8H, Cy). ^1H NMR (400.13 MHz, 253 K): δ 7.78 (d, $J_{\text{HP}} = 5$, 1H, CH), 6.61 (s, br, 1H, NH), 4.71, 4.65 (2s, $2 \times 5\text{H}$, Cp), 2.88 (m, 1H, Cy), 2.74, 2.50 (2 m, $2 \times 1\text{H}$, Cy), 2.24–1.42 (m, 8H, Cy). $^{13}\text{C}\{^1\text{H}\}$ NMR (100.62 MHz): δ 266.4 (s, $\mu\text{-CO}$), 214.4 (d, $J_{\text{CP}} = 21$, FeCO), 188.9 (s, CH), 85.0, 84.5 (2s, Cp), 49.8 [d, $J_{\text{CP}} = 22$, $\text{C}^1(\text{Cy})$], 31.9 [m, C^2 , $\text{C}^6(\text{Cy})$], 27.9 [d, $J_{\text{CP}} = 8$, $\text{C}^{3,5}(\text{Cy})$], 27.4 [d, $J_{\text{CP}} = 9$, $\text{C}^{5,3}(\text{Cy})$], 26.0 [s, $\text{C}^4(\text{Cy})$]. Spectroscopic data for **trans-7g**: ^1H NMR (400.13 MHz): δ 4.54, 4.37 (2s, $2 \times 5\text{H}$, Cp). ^1H NMR (400.13 MHz, 253 K): δ 8.21 (s, 1H, CH), 4.59, 4.43 (2s, $2 \times 5\text{H}$, Cp). $^{13}\text{C}\{^1\text{H}\}$ NMR (100.63 MHz): δ 88.1, 86.6 (2s, Cp); other resonances for this isomer were obscured by those of the major isomer.

Preparation of $[\text{Fe}_2\text{Cp}_2(\mu\text{-CyPNHNHCH})(\mu\text{-CO})(\text{CO})](\text{BF}_4)$ (8j). A slight excess of $\text{HBF}_4 \cdot \text{OEt}_2$ (16 μL of a 54% solution in Et_2O , 0.116 mmol) was added to a dichloromethane solution (5 mL) of compound **7g** (0.050 g, 0.110 mmol), and the mixture was stirred at room temperature for 5 min to give a red solution. The solvent was then removed under vacuum, and the residue was washed with Et_2O (3 \times 4 mL) and then petroleum ether (2 \times 4 mL) to give a mixture of the *cis* and *trans* isomers of complex **8j** as a red microcrystalline solid (0.058 g, 97%). The *cis/trans* ratio was measured to be 10:1 in CD_2Cl_2 solution. Anal. Calcd for $\text{C}_{19}\text{H}_{24}\text{BF}_4\text{Fe}_2\text{F}_4\text{N}_2\text{O}_2\text{P}$: C, 42.11; H, 4.46; N, 5.17. Found: C, 42.02; H, 4.52; N, 4.98. Spectroscopic data for **cis-8j**: ^1H NMR: δ 10.82 (dd, $J_{\text{HP}} = 19$, $J_{\text{HH}} = 4$, 1H, NH), 8.94 (dd, $J_{\text{HP}} = 6$, $J_{\text{HH}} = 4$, 1H, CH), 7.65 (s, br, 1H, PNH), 4.90, 4.86 (2s, $2 \times 5\text{H}$, Cp), 3.00 [m, 1H, $\text{HC}^1(\text{Cy})$], 2.71, 2.45 [2 m, $2 \times 1\text{H}$, $\text{HC}^2(\text{Cy})$], 2.21–1.49 (m, 8H, Cy). $^{13}\text{C}\{^1\text{H}\}$ NMR: δ 261.7 (d, $J_{\text{CP}} = 4$, $\mu\text{-CO}$), 220.4 (d, $J_{\text{CP}} = 16$, CH), 210.2 (d, $J_{\text{CP}} = 19$, FeCO), 86.3, 86.2 (2s, Cp), 49.9 [d, $J_{\text{CP}} = 24$, $\text{C}^1(\text{Cy})$], 32.3 [d, $J_{\text{CP}} = 6$, $\text{C}^{2,6}(\text{Cy})$], 32.0 [d, $J_{\text{CP}} = 6$, $\text{C}^{6,2}(\text{Cy})$], 27.9 [d, $J_{\text{CP}} = 10$, $\text{C}^{3,5}(\text{Cy})$], 27.4 [d, $J_{\text{CP}} = 11$, $\text{C}^{5,3}(\text{Cy})$], 26.0 [s, $\text{C}^4(\text{Cy})$]. Spectroscopic data for **trans-8j**: ^1H NMR: δ 10.69 (d, br, $J_{\text{HP}} = 16$, 1H, NH), 9.21 (dd, $J_{\text{HP}} = 6$, $J_{\text{HH}} = 4$, 1H, CH), 8.26 (s, br, 1H, PNH), 4.78, 4.67 (2s, $2 \times 5\text{H}$, Cp), 3.04–1.49 (m, 11H, Cy). $^{13}\text{C}\{^1\text{H}\}$ NMR: δ 88.8, 87.2 (2s, Cp); other resonances for this isomer were obscured by those of the major isomer.

Preparation of $[\text{Fe}_2\text{Cp}_2(\mu\text{-CyPNHNMeCH})(\mu\text{-CO})(\text{CO})](\text{I})$ (8k). Neat MeI (100 μL , 1.607 mmol) was added to a dichloromethane solution (5 mL) of compound **7g** (0.050 g, 0.110 mmol), and the mixture was stirred at room temperature for 1 h to give a red solution. The solvent was then removed under vacuum, and the residue was washed with petroleum ether (2 \times 4 mL) to give a mixture of the *cis* and *trans* isomers of complex

8k as a red microcrystalline solid (0.063 g, 95%). The *cis/trans* ratio in solution was measured to be 10:1 (CD₂Cl₂), 7:1 (CDCl₃), and 16:1 (Me₂CO-*d*₆). Anal. Calcd for C₂₀H₂₆Fe₂F₄N₂O₂P: C, 40.30; H, 4.40; N, 5.70. Found: C, 40.63; H, 4.52; N, 4.86. Spectroscopic data for *cis-8k*: ¹H NMR: δ 9.97 (s, 1H, CH), 8.50 (s, 1H, NH), 4.90, 4.82 (2s, 2 × 5H, Cp), 3.61 (s, 3H, Me), 3.13 (m, 1H, Cy), 2.66–1.70 (m, 10H, Cy). ¹³C{¹H} NMR (Me₂CO-*d*₆): δ 263.3 (s, μ-CO), 222.2 (d, *J*_{CP} = 18, CH), 212.8 (d, *J*_{CP} = 20, FeCO), 87.2, 86.9 (2s, Cp), 49.6 [d, *J*_{CP} = 23, C¹(Cy)], 48.7 (s, Me), 32.3 [m, C², C⁶(Cy)], 28.3 [d, *J*_{CP} = 12, C^{3,5}(Cy)], 27.6 [d, *J*_{CP} = 13, C^{5,3}(Cy)], 26.2 [s, C⁴(Cy)]. Spectroscopic data for *trans-8k*: ¹H NMR: δ 10.44 (s, 1H, CH), 8.74 (s, 1H, NH), 4.82, 4.76 (2s, 2 × 5H, Cp), 3.71 (s, 3H, Me), 2.66–1.70 (m, 11H, Cy).

Preparation of [Fe₂Cp₂(μ-Mes*PN₂CH(CO₂Et))(μ-CO)] (9). A toluene solution (5 mL) of compound **2c.2** (0.060 g, 0.084 mmol) was irradiated with visible–UV light in a quartz Schlenk tube while keeping a gentle N₂ (99.9995%) purge at 288 K for 50 min to give a green solution. The solvent was then removed under vacuum, and the residue was dissolved in a minimum of dichloromethane–petroleum ether (1:8) and chromatographed through an alumina column (activity IV) at 263 K. Elution with the same solvent mixture yielded a red fraction containing some [Fe₂Cp₂(CO)₄]. Elution with dichloromethane–petroleum ether (1:3) yielded a green fraction. Removal of solvents under vacuum from this fraction gave compound **9** as a green microcrystalline solid (0.049 g, 85%). The crystals used in the diffractometric study were grown from a concentrated petroleum ether solution of the complex at 253 K. Anal. Calcd for C₃₄H₄₅Fe₂N₂O₄P: C, 59.32; H, 6.59; N, 4.07. Found: C, 59.13; H, 6.56; N, 3.88. ¹H NMR (400.13 MHz): δ 7.34 (d, *J*_{HP} = 2, 2H, C₆H₂), 6.22 (s, 1H, CH), 4.74, 4.72 (2s, 2 × 5H, Cp), 4.00 (q, *J*_{HH} = 7, 2H, OCH₂), 1.42 (s, 18H, *o*-^{*t*}Bu), 1.27 (s, 9H, *p*-^{*t*}Bu), 1.10 (t, *J*_{HH} = 7, 3H, Me). ¹³C{¹H} NMR (100.62 MHz): δ 279.9 (d, *J*_{CP} = 25, μ-CO), 164.5 (s, CO₂Et), 155.1 [s, C²-(C₆H₂)], 154.0 [s, C⁴(C₆H₂)], 134.4 [d, *J*_{CP} = 37, C¹(C₆H₂)], 133.9 (d, *J*_{CP} = 27, CH), 122.6 [d, *J*_{CP} = 12, C³(C₆H₂)], 89.9 (d, *J*_{CP} = 2, Cp), 85.3 (s, Cp), 60.7 (s, OCH₂), 38.0 [s, C¹(*o*-^{*t*}Bu)], 32.9 [s, C²(*o*-^{*t*}Bu)], 32.4 [s, C¹(*p*-^{*t*}Bu)], 31.1 [s, C²(*p*-^{*t*}Bu)], 14.3 (s, Me).

X-ray Structure Determination of Compounds 2a.1 and 3. The X-ray intensity data were collected on a Smart-CCD-1000 Bruker diffractometer using graphite-monochromated Mo K α radiation at 120 K. Cell dimensions and orientation matrixes were initially determined from least-squares refinements on reflections measured in three sets of 30 exposures collected in three different ω regions and eventually refined against all reflections. The software SMART³⁶ was used for collecting frames of data, indexing reflections, and determining lattice parameters. The collected frames were then processed for integration by the software SAINT,³⁶ and a multiscan absorption correction was applied with SADABS.³⁷ Using the program suite WinGX,³⁸ the structure was solved by Patterson interpretation and phase expansion and refined with full-matrix least-squares on *F*² using SHELXL97.³⁹ All non-hydrogen atoms were refined anisotropically. All hydrogen atoms were fixed at calculated geometric positions in the last least-squares refinements, except for H(4a) and H(4b) (for compound **2a.1**) and H(2), H(14a), and H(14b) (for compound **3**), which were located

in the Fourier maps. All hydrogen atoms were given an overall isotropic thermal parameter. Further details of the data collection and refinements are given in Table 6.

X-ray Structure Determination of Compound 7e. The X-ray intensity data were collected on a Kappa-Apex-II Bruker diffractometer using graphite-monochromated Mo K α radiation at 100 K. The software APEX⁴⁰ was used for collecting frames with the omega/phi scan measurement method. The Bruker SAINT software was used for the data reduction,³⁶ and a multiscan absorption correction was applied with SADABS.³⁷ Using the program suite WinGX,³⁸ the structure was solved by Patterson interpretation and phase expansion and refined with full-matrix least-squares on *F*² using SHELXL97.³⁹ Two independent molecules were found to be present in the asymmetric unit. The FeCp moiety, the cyclohexyl group, and O(34) and C(36) atoms on the second independent molecule were highly disordered and were modeled in two positions (occupancy factor = 0.5/0.5, except for C(36) = 0.6/0.4). Non-H atoms were refined anisotropically except for a number of atoms involved in the disorder, which were refined isotropically because some of their temperature factors were persistently non-positive definites. Not all hydrogen atoms were found in Fourier maps, so all hydrogen atoms were fixed at calculated geometric positions in the last least-squares refinements, except for the N–H atoms (H(1) and H(3)), which could be located in the Fourier maps, and their positions were refined satisfactorily. All hydrogen atoms were given an overall isotropic thermal parameter. Further details of the data collection and refinements are given in Table 6.

X-ray Structure Determination of Compound 9. Data collection was performed on an Oxford Diffraction Xcalibur Nova single-crystal diffractometer, using Cu K α radiation. Images were collected at a 65 mm fixed crystal–detector distance, using the oscillation method, with 1° oscillation and variable exposure time per image (1–30 s). Data collection strategy was calculated with the program CrysAlis Pro CCD.⁴¹ Data reduction and cell refinement were performed with the program CrysAlis Pro RED.⁴¹ An empirical absorption correction was applied using the SCALE3 ABSPACK algorithm as implemented in the program CrysAlis Pro RED.⁴¹ Using the program suite WinGX,³⁸ the structure was solved by direct methods and refined with full-matrix least-squares on *F*² using SHELXL97.³⁹ This compound was found to crystallize with half a molecule of hexane placed on an element of symmetry described by the operation $-x+3/2, -y+3/2, -z+1$. During the final stages of the refinement, all the positional parameters and the anisotropic temperature factors of all the non-H atoms were refined anisotropically. All hydrogen atoms were geometrically placed and refined using a riding model, except for H(13), which was located in the Fourier maps and refined isotropically. Further details of the data collection and refinements are given in Table 6.

Acknowledgment. We thank the DGI of Spain (Projects CTQ2006-01207 and CTQ2009-09444) and the COST action CM0802 “PhoSciNet” for supporting this work, and the MEC of Spain for a grant (to R.G.).

Supporting Information Available: CIF file giving the crystallographic data for the structural analysis of compounds **2a.1**, **3**, **7e**, **7f**, and **9**. This material is available free of charge via the Internet at <http://pubs.acs.org>.

(36) SMART & SAINT Software Reference Manuals, Version 5.051 (Windows NT Version); Bruker Analytical X-ray Instruments: Madison, WI, 1998.

(37) Sheldrick, G. M. *SADABS, Program for Empirical Absorption Correction*; University of Göttingen: Göttingen, Germany, 1996.

(38) Farrugia, L. J. *J. Appl. Crystallogr.* **1999**, *32*, 837.

(39) Sheldrick, G. M. *Acta Crystallogr., Sect. A* **2008**, *64*, 112.

(40) APEX 2, version 2.0-1; Bruker AXS Inc: Madison, WI, 2005.

(41) CrysAlis Pro; Oxford Diffraction Ltd.: Oxford, U.K., 2006.